

Cooperativity and Oligomeric Status of Cardiac Muscarinic Cholinergic Receptors[†]Paul S.-H. Park,[‡] Chi Shing Sum,[§] Asha B. Pawagi,[‡] and James W. Wells^{*,‡,§}

Faculty of Pharmacy and Department of Pharmacology, University of Toronto, Toronto, Ontario, Canada M5S 2S2

Received August 31, 2001; Revised Manuscript Received December 20, 2001

ABSTRACT: Muscarinic cholinergic receptors can appear to be more numerous when labeled by [³H]quinuclidinylbenzilate (QNB) than by *N*-[³H]methylscopolamine (NMS). The nature of the implied heterogeneity has been studied with M₂ receptors in detergent-solubilized extracts of porcine atria. The relative capacity for [³H]NMS and [³H]QNB was about 1 in digitonin–cholate, 0.56 in cholate–NaCl, and 0.44 in Lubrol-PX. Adding digitonin to extracts in cholate–NaCl increased the absolute capacity for both radioligands, and the relative capacity increased to near 1. The latency cannot be attributed to a chemically impure radioligand, instability of the receptor, an irreversible effect of NMS, or a failure to reach equilibrium. Binding at near-saturating concentrations of [³H]QNB in cholate–NaCl or Lubrol-PX was blocked fully by unlabeled NMS, which therefore appeared to inhibit noncompetitively at sites inaccessible to radiolabeled NMS. Such an effect is inconsistent with the notion of functionally distinct, noninterconverting, and mutually independent sites. Both the noncompetitive effect of NMS on [³H]QNB and the shortfall in capacity for [³H]NMS can be described quantitatively in terms of cooperative interactions within a receptor that is at least tetravalent; no comparable agreement is possible with a receptor that is only di- or trivalent. The M₂ muscarinic receptor therefore appears to comprise at least four interacting sites, presumably within a tetramer or larger array, and ligands appear to bind in a cooperative manner under at least some conditions.

G protein-coupled receptors are known to occur as oligomers (1–3). The existence of homooligomers has been suggested by several lines of evidence and substantiated by the coimmunoprecipitation of differently tagged receptors from extracts of cells expressing both proteins. Aggregates identified in this manner include oligomers of the M₂ and M₃ muscarinic receptors (4, 5), the β_2 -adrenergic receptor (6), the D₃ dopamine receptor (7), the δ -opioid receptor (8), the somatostatin SST2A receptor (9), and the α -factor receptor (10). The occurrence of homooligomers in whole cells has been demonstrated by means of energy transfer (FRET¹ and BRET) in studies on somatostatin receptors (11), β -adrenergic receptors (12), and δ -opioid receptors (13) in mammalian cells and on the α -factor receptor in yeast (14).

Heterooligomers have been comparatively elusive, and attempts at coimmunoprecipitation have failed to identify a mixed complex of M₂ muscarinic and β_2 -adrenergic receptors (6) or of a modified M₃ muscarinic receptor and the M₁

receptor, the M₂ receptor, or the V2 vasopressin receptor (5). While such examples indicate that aggregation is selective, heteromeric complexes have been shown to form between the R1 and R2 forms of the GABA_B receptor (15–19), the δ - and κ -opioid receptors (20), the μ - and δ -opioid receptors (21), the somatostatin SST2A and SST3 receptors (9), the AT₁ and bradykinin B₂ receptors (22), and the dopamine D₁ and adenosine A₁ receptors (23). Heteromeric complexes of the D₂ dopamine receptor and somatostatin SST5 receptor also have been detected by photobleaching FRET in CHO-K1 cells (24).

A functional role for oligomers is implied by the distinct properties that can emerge from the coexpression of two isoforms. Membranes from COS-7 cells transfected with the genes for two complementary chimeras of the α_2 -adrenergic and M₃ muscarinic receptors were found to bind adrenergic or muscarinic antagonists only when the recombinant proteins were coexpressed, which also led to the carbachol-stimulated hydrolysis of phosphatidylinositol (25). Similarly, the K102A and K199A mutants of the angiotensin AT_{1A} receptor bound peptidic agonists and the antagonist [³H]DuP753 only when coexpressed, and the maximal effect occurred when the two genes were transfected in equal amounts. In that case, recovery of binding was not accompanied by recovery of a receptor-mediated response (26). A constitutively desensitized mutant of the β_2 -adrenergic receptor has been shown to regain the native stimulatory effect on adenylate cyclase when coexpressed with the wild-type receptor (27). Coexpression of the human PAF receptor with four dysfunctional mutants variously inhibited binding and surface expression, increased constitutive activity, and altered the PAF-induced

[†] This investigation was supported by the Heart and Stroke Foundation of Ontario (T2970 and T3769) and The Medical Research Council of Canada (MT14171).

* Address correspondence to this author at the Faculty of Pharmacy, University of Toronto, 19 Russell St., Toronto, Ontario, Canada M5S 2S2. Telephone: (416) 978-3068. Facsimile: (416) 978-8511. E-mail: jwells@phm.utoronto.ca.

[‡] Faculty of Pharmacy, University of Toronto.

[§] Department of Pharmacology, University of Toronto.

¹ Abbreviations: BRET, bioluminescence resonance energy transfer; FRET, fluorescence resonance energy transfer; FTIR, Fourier transform infrared; GMP-PNP, guanylyl imidodiphosphate; HEPES, sodium *N*-(2-hydroxyethyl)piperazine-*N'*-2-ethanesulfonate; NMS, *N*-methylscopolamine; PAF, platelet-activating factor; QNB, (–)-quinuclidinylbenzilate; PMSF, phenylmethanesulfonyl fluoride.

production of inositol phosphates (28). Oligomers therefore appear to have distinct implications for binding on one hand and for efficacy or intrinsic activity on the other.

Early reports of multimeric forms attracted little attention, owing in part to the prevailing view of G protein-mediated systems: namely, that the receptors are mutually independent and that signaling involves a ligand-regulated interconversion between free receptor (R) and free G protein or subunits thereof on one hand and a 1:1 heteromeric RG complex on the other (e.g., refs 29–32). Such an arrangement also is invoked to account for the nucleotide-sensitive dispersion of affinities revealed in the binding of agonists, a characteristic and almost universal pattern that reflects in part the influence of the G protein (29, 33, 34). The origin of the dispersion is of mechanistic interest, since its breadth correlates with properties of the response such as efficacy and intrinsic activity in muscarinic and other G protein-mediated systems (e.g., refs 35–37).

The notion that multiple states of affinity are induced by the G protein in an otherwise homogeneous population of mutually independent sites is problematic in some respects, and it is particularly difficult to sustain on quantitative grounds (e.g., refs 38 and 39 and references cited therein). An alternative explanation is suggested by the evidence for oligomers and the attendant possibility of cooperative interactions, which can account for effects that resist a mechanistically consistent explanation in other terms (40). In the present report, we describe a pattern of noncompetitive and apparently cooperative effects in the binding of antagonists to M_2 muscarinic receptors in detergent-solubilized extracts of porcine atria. The data are shown to be inconsistent with the notion of distinct, mutually independent, and noninterconverting sites but can be described in terms of cooperative interactions within a receptor that is at least tetraivalent.

MATERIALS AND METHODS

Ligands, Detergents, and Other Materials. *N*-[3 H]Methylscopolamine was purchased as the chloride salt from NEN Life Science Products (lot 3406009, 83.5 Ci/mmol) and as the bromide salt from Amersham Pharmacia Biotech (batch 27, 78.3 Ci/mmol). Scopolamine was absent from both batches of *N*-[3 H]methylscopolamine as indicated by mass spectra provided by the manufacturers and, in the case of the product from NEN, obtained at the Mass Spectrometry Laboratory, Molecular Medicine Research Centre, University of Toronto. (–)-[3 H]Quinuclidinylbenzilate was purchased from NEN (lots 3329455 and 3329907, 42 Ci/mmol) and Amersham (batch 44, 48 Ci/mmol). Unlabeled *N*-methylscopolamine hydrobromide was purchased from Sigma-Aldrich. Scopolamine hydrobromide, unlabeled (R)-(–)-quinuclidinylbenzilate, and (S)-(+)-quinuclidinylbenzilate were purchased from RBI-Sigma.

Digitonin usually was obtained from Wako Bioproducts at a purity near 100%; material of lower purity was obtained on occasion from Boehringer Mannheim (>75%, 93%) and Calbiochem (>75%). The latter products were used primarily to elute the columns of Sephadex G-50 during the binding assays. Sodium cholate and Lubrol-PX (polyoxyethylene-9-lauryl ether, polidocanol) were purchased from Sigma-Aldrich. Solubilized receptor was concentrated as required

by means of Centricon-10 and Centriprep-30 filters (Amicon) purchased from Millipore.

HEPES was obtained as the free base from Boehringer Mannheim. EDTA and EGTA were obtained as the free acids from British Drug Houses or Bioshop Canada. Bacitracin, all protease inhibitors, and Sephadex G-50 were from Sigma-Aldrich. Protein was estimated by the Lowry method using reagents and bovine serum albumin, taken as the standard, purchased from Pierce.

Soluble Preparations of M_2 Muscarinic Receptor. Sarcolemmal membranes were collected from a sucrose gradient and spun down in buffer A² essentially as described previously (39). The gradient typically yielded 90–120 mg of protein from about 350 g of left plus right atria. The sarcolemmal membranes were washed twice to remove imidazole and endogenous ligands. The washing buffer was the same as that to be used in subsequent steps (i.e., buffer B for later solubilization in digitonin–cholate or Lubrol-PX; buffer C for solubilization in cholate–NaCl). The product from the sucrose gradient was suspended in the appropriate buffer (120 mL) with one burst of a Brinkmann Polytron (setting 5, 5 s), and the suspension then was centrifuged for 40 min at 4 °C and 100000g. This step was repeated, and the pellets from the second spin were stored at –70 °C.

Solubilization in digitonin–cholate or Lubrol-PX was carried out in a single extraction as described by Peterson et al. (41). Frozen membranes were thawed on ice and suspended in buffer B (5.5 mg of protein/mL) by means of the Polytron (setting 5, 5 s). Detergent then was added from a stock solution prepared at 10 times the final concentration, also in buffer B. The suspension was shaken on a horizontal shaker for 10 min at room temperature and then centrifuged for 40 min at 4 °C and 100000g. The supernatant fraction was stored on ice until required for the binding assays. The final concentration of digitonin and Lubrol-PX was 1.1%; that of cholate accompanying digitonin was 0.06%.

Solubilization in sodium cholate plus NaCl was carried out according to a procedure modified from that described by Carson (42). Washed sarcolemmal membranes were thawed on ice and suspended in buffer D (2 mg of protein/mL), and the mixture was shaken for 1 h at room temperature. The suspension then was diluted 1:1 with a buffer (40 mM NaH_2PO_4 , 1 mM EGTA, adjusted to pH 7.40 with NaOH) and centrifuged for 40 min at 4 °C and 100000g. The supernatant fraction was stored on ice until required for the binding assays. The final concentrations of cholate and NaCl were 0.08% and 0.5 M, respectively.

Extracts prepared in cholate–NaCl were supplemented with digitonin by adding an aliquot of buffer B containing digitonin at 16 times the final concentration of 0.4%. Controls were prepared by adding an equal aliquot of buffer B alone.

² Buffer solutions: buffer A (39), 20 mM imidazole, 1 mM $\text{Na}_2\text{-EDTA}$, 0.1 mM PMSF, 0.02% (w/v) sodium azide, 1 mM benzamidine, 2 $\mu\text{g/mL}$ pepstatin A, 0.2 $\mu\text{g/mL}$ leupeptin, 200 $\mu\text{g/mL}$ bacitracin, pH 7.60, with HCl; buffer B, 20 mM KH_2PO_4 , 20 mM NaCl, 1 mM EDTA, 0.1 mM PMSF, pH 7.40, with NaOH; buffer C, 20 mM NaH_2PO_4 , 20 mM NaCl, 1 mM EGTA, 0.1 mM PMSF, pH 7.40, with NaOH; buffer D, 40 mM NaH_2PO_4 , 1 M NaCl, 1 mM EGTA, 0.16% sodium cholate, 0.1 mM PMSF, pH 7.40, with NaOH; buffer E, 20 mM HEPES, 20 mM NaCl, 1 mM EDTA, 5 mM MgSO_4 , 0.1 mM PMSF, pH 7.40, with NaOH; buffer F, 20 mM HEPES, 20 mM NaCl, 1 mM EDTA, 5 mM MgSO_4 , pH 7.40, with NaOH.

The concentrations of cholate and NaCl therefore were reduced slightly to 0.075% and 0.47 M, respectively.

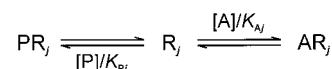
Binding Assays. Ligands were dissolved in buffer E supplemented with the detergent used to solubilize the receptor. The concentration of digitonin, cholate, or Lubrol-PX was 0.1%, and digitonin was accompanied by 0.02% cholate. For binding to solubilized receptor in digitonin–cholate or Lubrol-PX, 50 μ L of a solution containing all of the ligands was added to 3 μ L of the solubilized preparation in polypropylene microcentrifuge tubes. In cholate–NaCl, 43 or 33 μ L of ligand-containing solution was added to 10 or 20 μ L of receptor, respectively. Except where stated otherwise, the reaction mixture was incubated for 45 min when only *N*-methylscopolamine was present and for 2 h when the mixture contained quinuclidinylbenzilate. The temperature of incubation was 30 °C throughout. The reaction was terminated, and the bound radioligand was separated by applying an aliquot of the sample (50 μ L) to a column of Sephadex G-50 fine (0.8 \times 6.5 cm). The column was preequilibrated and eluted with buffer F supplemented with digitonin, cholate, or Lubrol-PX at a concentration of 0.017%. All of the eluant up to and including the void volume was collected (1.45 mL) and assayed for radioactivity. Additional details have been described elsewhere (39). Binding assays generally were carried out within 1 week of solubilization.

Assays were performed in duplicate or triplicate. Each sample was counted twice by liquid scintillation spectrometry (Beckman LS7800, Beckman LS5000, or Packard 2100TR), and the individual values were averaged to obtain the mean and standard error used in subsequent analyses. Absolute count rates were determined by means of an external standard. To compare the relative apparent capacity of a preparation for *N*-[³H]methylscopolamine and [³H]quinuclidinylbenzilate, binding was measured at graded concentrations of both radioligands taken in parallel. Nonspecific binding was taken throughout as total binding in the presence of 1 mM unlabeled *N*-methylscopolamine.

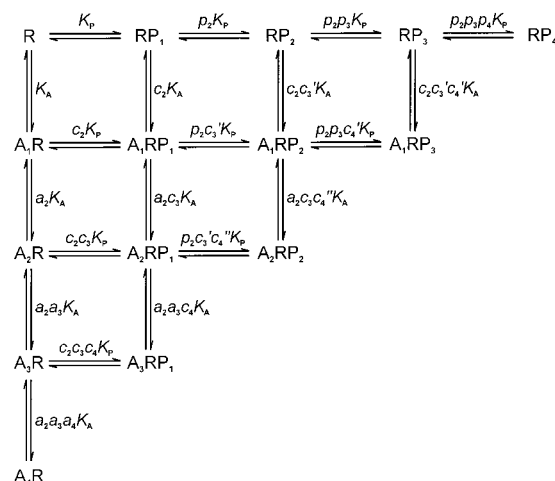
Analysis of Data. All data were analyzed with total binding taken as the dependent variable (B_{obsd}) and with the total concentrations of all ligands taken as the independent variables. Any subsequent manipulations were for the purpose of presentation only and did not alter the relationship between the data and the fitted curve. Except where stated otherwise, levels of specific binding (B_{sp}), estimates of total receptor ($[R]_t$), and estimates of maximal specific binding (B_{max}) are presented as the concentration in the binding assay (pM); the concentrations of ligands denote the total molar concentration in the binding assay. With both [³H]quinuclidinylbenzilate and *N*-[³H]methylscopolamine, nonspecific binding increased linearly with the concentration of unbound radioligand.

Data acquired at graded concentrations of [³H]quinuclidinylbenzilate or *N*-[³H]methylscopolamine were analyzed empirically according to eq 1 (i.e., the Hill equation), in which $[P]_t$ represents the total concentration of the radioligand. The quantity B_{sp} represents total specific binding at the corresponding value of $[P]_t$, and the parameter B_{max} represents maximal specific binding; the parameter EC_{50} represents the value of $[P]$ that yields half-maximal occupancy, and n_H is the corresponding Hill coefficient. The parameter NS represents the fraction of unbound radioligand

Scheme 1



Scheme 2



that appears as nonspecific binding. Equation 1 was solved numerically in the manner described previously (cf. eq 204 in ref 43).

$$B_{\text{obsd}} = B_{\text{max}} \frac{([P]_t - B_{\text{sp}})^{n_H}}{EC_{50}^{n_H} + ([P]_t - B_{\text{sp}})^{n_H}} + NS([P]_t - B_{\text{sp}}) \quad (1)$$

Mechanistic descriptions of the data were based on the notions of intrinsic heterogeneity (Scheme 1) and cooperativity (Scheme 2). Estimates of total binding were fitted according to the equation $B_{\text{obsd}} = B_{\text{sp}} + NS([P]_t - B_{\text{sp}})$, in which the different quantities are as described above. The value of B_{sp} was computed according to Scheme 1 or Scheme 2.

Scheme 1 represents a multisite model in which the radioligand (P) and an unlabeled ligand (A) compete for distinct and mutually independent sites (R_j , $j = 1, 2, \dots, n$). Sites of type j bind P and A with equilibrium dissociation constants K_{Pj} and K_{Aj} , respectively, and constitute the fraction F_j of all sites (i.e., $F_j = [R_j]_t/[R]_t$, where $[R_j]_t = [R_j] + [AR_j] + [PR_j]$ and $[R]_t = \sum_{j=1}^n [R_j]_t$). Total specific binding of the probe was calculated according to eq 2, and the required values of $[PR_j]$ were obtained as described below.

$$B_{\text{sp}} = \sum_{j=1}^n [PR_j] \quad (2)$$

Cooperativity was modeled according to Scheme 2 and similar models, in which a multivalent receptor (R) can bind up to 2, 3, 4, 6, or 8 equiv of either A or P. The receptor presumably is oligomeric, and it is assumed that the quaternary structure remains formally intact under the conditions of the binding assays; that is, there is no exchange of individual subunits within the system. The models therefore can accommodate processes in which dissociated monomers regroup without exchanging partners. Asymmetry cannot be detected with the present data, and all sites of the vacant oligomer (R) are assumed to bind the radioligand (P) or the unlabeled ligand (A) with the microscopic dissociation

constant K_P or K_A , respectively (e.g., $K_P = [P][R]/[PR]$). The parameters p_j and a_j represent the cooperativity factors for binding of the j th equivalent of P or A to form RP_j or A_jR ($j \geq 2$) (e.g., $[RP_{j-1}][P]/[RP_j] = \prod_{i=2}^j p_i K_P$); the parameters c_j , c'_j , and c''_j represent cooperativity factors in the formation of mixed complexes.

Total specific binding was calculated according to eq 3 for binding to a dimer, trimer, tetramer (Scheme 2), hexamer, or octamer, where i and j are the i th and j th equivalents of P and A, respectively, and n is the total number of interacting sites. The species A_0RP_i is denoted as RP_i in Scheme 2 and in eqs 3a–c, which are the expansions of eq 3 for a dimer, trimer, and tetramer, respectively. Coefficients greater than 1 represent the degree of occupancy by P, since R is defined as multivalent, times the number of possible combinations involving two ligands and two or more interacting sites. Stoichiometrically equivalent states are indistinguishable with the present data, and the microscopic dissociation constant therefore was taken as the same for all vacant sites on partially liganded R (e.g., $[P][POOA]/[PPOA] = [P][POOA]/[POPA]$ in Scheme 2, where "O" represents a vacant site on tetravalent R). Further details concerning the formulation of cooperative models have been described elsewhere (40, 43).

$$B_{sp} = \sum_{i=1}^n \sum_{j=0}^{n-i} i \binom{n}{i} \binom{n-i}{j} [A_j RP_i] \quad (3)$$

$$B_{sp} = 2[RP_1] + 2[RP_2] + 2[A_1 RP_1] \quad (3a)$$

$$B_{sp} = 3[RP_1] + 6[RP_2] + 3[RP_3] + 6[A_1 RP_1] + 3[A_2 RP_1] + 6[A_1 RP_2] \quad (3b)$$

$$B_{sp} = 4[RP_1] + 12[RP_2] + 12[RP_3] + 4[RP_4] + 12[A_1 RP_1] + 12[A_2 RP_1] + 24[A_1 RP_2] + 12[A_2 RP_2] + 4[A_3 RP_1] + 12[A_1 RP_3] \quad (3c)$$

The value of B_{sp} in eqs 2 and 3 was calculated from the expansions in terms of the total concentration of R and the free concentrations of A and P. The latter were computed numerically from the corresponding implicit equations for $[A]_t$ and $[P]_t$ as described previously (39, 40, 43).

The results of analyses involving multiple sets of data from replicated experiments have been presented throughout with reference to a single fitted curve. To obtain the values plotted on the y-axis, estimates of B_{obsd} were adjusted according to the expression $B'_{obsd} = B_{obsd} \{f(\bar{\mathbf{x}}_i, \bar{\mathbf{a}})/f(\mathbf{x}_i, \mathbf{a})\}$. The function f represents the fitted model. The vectors \mathbf{x}_i and \mathbf{a} represent the independent variables at point i and the fitted parameters for the set of data under consideration; $\bar{\mathbf{x}}_i$ and $\bar{\mathbf{a}}$ are the corresponding vectors in which values that differ from experiment to experiment have been replaced by the means for experiments associated with the fitted curve. Individual values of B'_{obsd} at the same \mathbf{x}_i were averaged to obtain the mean and standard error plotted in the figure. The y-axis represents specific binding (B_{sp}) throughout: that is, the value of B'_{obsd} less the fitted estimate of nonspecific binding at the same concentration of unbound radioligand (44).

Statistical Procedures. All parameters were estimated by nonlinear regression, and values at successive iterations of the fitting procedure were adjusted according to the algorithm of Marquadt (45). Affinities and cooperativity factors were

optimized throughout on a logarithmic scale (i.e., $\log K_P$, $\log K_P$, $\log p_j$, etc.). Most analyses involved multiple sets of data, and specific details regarding the assignment of shared parameters are described where appropriate. Values of $[R]_t$ were assigned separately to data from separate experiments; values of NS generally were common to all data acquired with the same radioligand in the same experiment.

Weighting of the data, tests for significance, and other statistical procedures were performed as described elsewhere (43, 46). Weighted residuals were of comparable magnitude within each set of data. In simultaneous analyses, individual sets of data generally made comparable contributions to the total weighted sum of squares; thus, the fits were not dominated by the data from one experiment or group of experiments. Mean values calculated from two or more individual estimates of a parameter or other quantity are presented together with the standard error. For parametric values derived from a single analysis of one or more sets of data, the errors were estimated from the diagonal elements of the covariance matrix. Such values reflect the range within which the weighted sum of squares is essentially the same.

RESULTS

Latent Sites and Differential Capacity for Muscarinic Antagonists. With some detergents, extracts of sarcolemmal membranes can appear to contain more sites for $[^3H]$ -quinuclidinylbenzilate than for N - $[^3H]$ methylscopolamine. The relative apparent capacity for N - $[^3H]$ methylscopolamine and $[^3H]$ quinuclidinylbenzilate was 0.56 ± 0.04 and 0.44 ± 0.06 when membranes were extracted with cholate–NaCl and Lubrol-PX, respectively (Figure 1A,C, Table 1). The relative capacity in cholate–NaCl was near 0.5 when measured within a few days of solubilization and increased to about 0.75 after storage at 0 °C for 7 days or more. The value was the same with radioligands from either NEN Life Science Products or Amersham Pharmacia Biotech. Up to about 50% of the receptors therefore appear to be of anomalously weak affinity for N - $[^3H]$ methylscopolamine under some conditions.

With receptor solubilized in digitonin–cholate, the relative apparent capacity for N - $[^3H]$ methylscopolamine and $[^3H]$ -quinuclidinylbenzilate was near or equal to 1 (Figure 2A, Table 1). There was no change when NaCl was added directly to the extracts in order to increase the salt concentration to that used for extraction in cholate–NaCl (i.e., 0.5 M). The relative apparent capacity increased from 0.5 to about 1 when digitonin was added to extracts prepared in cholate–NaCl (Figure 2C, Table 1). To assess the effect of digitonin in absolute terms, the original extract and the digitonin-supplemented preparation were characterized in parallel for the binding of $[^3H]$ quinuclidinylbenzilate. In seven such experiments on preparations in cholate–NaCl, digitonin increased the apparent capacity 1.4–2.1-fold. Since the relative apparent capacity for N - $[^3H]$ methylscopolamine and $[^3H]$ quinuclidinylbenzilate was near 1 in digitonin-supplemented preparations, the apparent capacity for N - $[^3H]$ -methylscopolamine increased by as much as 4-fold upon the addition of digitonin. Muscarinic receptors therefore can be solubilized in at least two latent forms, one of which binds neither radioligand and one of which binds only $[^3H]$ -quinuclidinylbenzilate at the concentrations used in the

Table 1: Empirical Characterization of Specific Binding^a

preparation	<i>N</i> -[³ H]methylscopolamine			[³ H]quinuclidinylbenzilate			$B_{\max, [^3\text{H}]\text{NMS}} / B_{\max, [^3\text{H}]\text{QNB}}$
	log EC ₅₀	<i>n</i> _H	<i>B</i> _{max} (pM)	log EC ₅₀	<i>n</i> _H	<i>B</i> _{max} (pM)	
digitonin–cholate (11)	-8.25 ± 0.12	1.00 ± 0.06	80–604	-9.01 ± 0.12	0.94 ± 0.07	92–632	0.90 ± 0.05
cholate–NaCl (8) ^b	-8.39 ± 0.12	1.01 ± 0.07	101–246	-9.39 ± 0.10	0.91 ± 0.08	138–353	0.56 ± 0.04
cholate–NaCl plus digitonin (3)	-8.21 ± 0.10	0.91 ± 0.04	342–365	-9.14 ± 0.07	1.08 ± 0.05	329–402	0.96 ± 0.04
Lubrol-PX (6)	-7.24 ± 0.10	1.00 ± 0.08	99–322	-7.65 ± 0.05	0.97 ± 0.06	195–580	0.44 ± 0.06

^a Binding was measured at graded concentrations of [³H]NMS and [³H]QNB, as illustrated in the left-hand panels of Figures 1 and 2. The two radioligands were used in parallel in each experiment, and the number of experiments is shown in parentheses. Data from individual experiments were analyzed in terms of eq 1 to obtain estimates of *n*_H, log EC₅₀, and *B*_{max} for each radioligand. The relative capacity for [³H]NMS and [³H]QNB was calculated for each experiment (i.e., $B_{\max, [^3\text{H}]\text{NMS}} / B_{\max, [^3\text{H}]\text{QNB}}$), and the individual estimates of log EC₅₀, *n*_H, and relative capacity were averaged to obtain the means (±SEM) listed in the table. The values of *B*_{max} indicate the concentration in the binding assay. ^b The means listed in the table include values from two experiments that were performed more than 7 days after solubilization and in which the relative capacity was about 0.75. If those values are excluded from the average, the results are as follows (*N* = 6): [³H]NMS, log EC₅₀ = -8.46 ± 0.14, *n*_H = 0.98 ± 0.09; [³H]QNB, log EC₅₀ = -9.46 ± 0.08, *n*_H = 0.89 ± 0.10; $B_{\max, [^3\text{H}]\text{NMS}} / B_{\max, [^3\text{H}]\text{QNB}}$ = 0.50 ± 0.02.

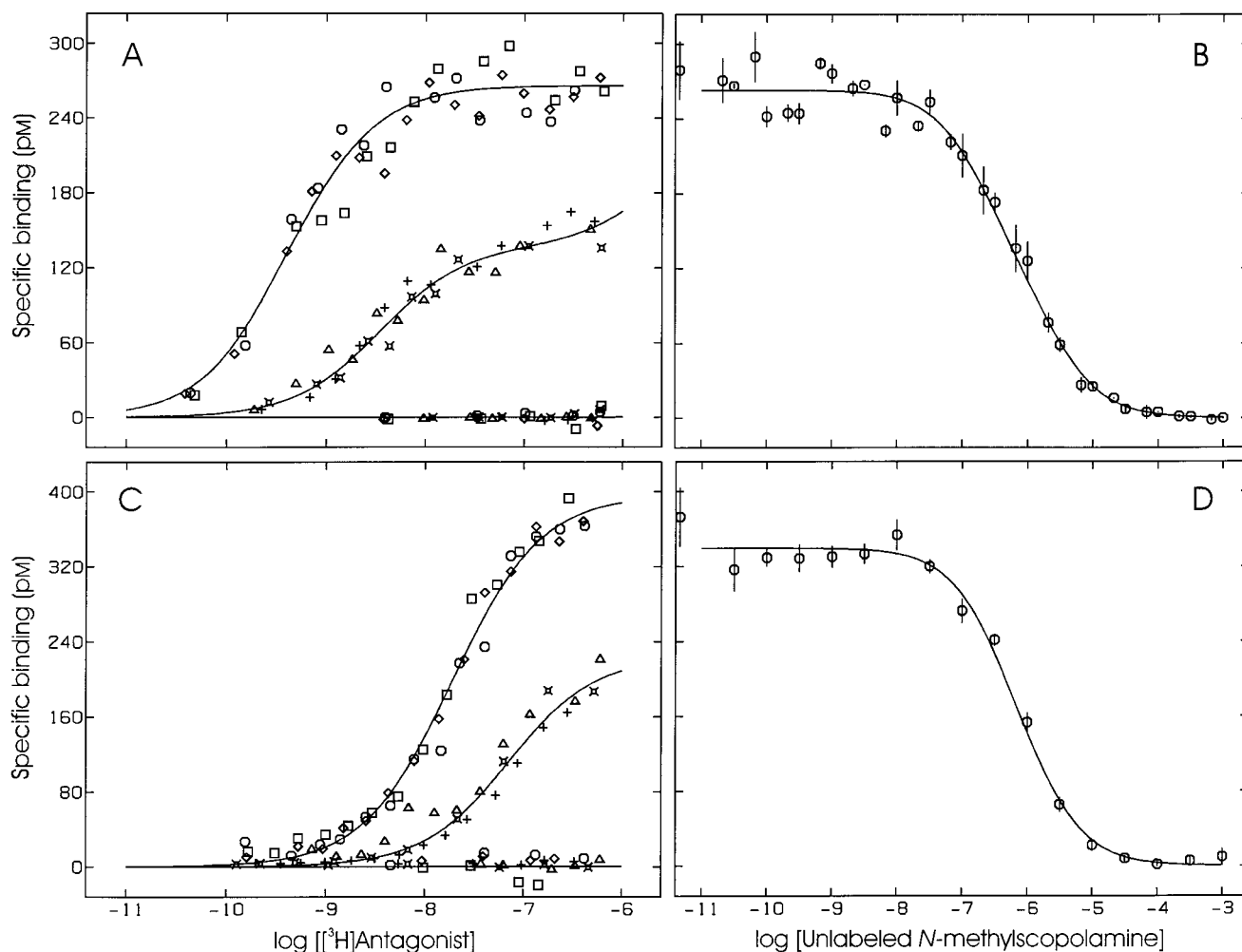


FIGURE 1: Binding to M₂ receptors in cholate–NaCl and in Lubrol-PX. Sarcolemmal membranes were solubilized in cholate–NaCl (A, B) or Lubrol-PX (C, D). (A, C) Total binding was measured at graded concentrations of [³H]QNB (○, ◇, □) and [³H]NMS (△, ◊, +), either alone (upper curves) or in the presence of 1 mM unlabeled NMS (baseline). The results from six independent experiments are shown (A, *N* = 3; C, *N* = 3), and different symbols denote data from different experiments (○, △; ◇, ◊; □, +). (B, D) Total binding was measured at a near-saturating concentration of [³H]QNB and graded concentrations of unlabeled NMS (B, *N* = 4; D, *N* = 3). The lines represent the best fits of eq 2 to the pooled data from the seven experiments represented in panels A and B and, in a separate analysis, to the pooled data from the six experiments represented in panels C and D. The parametric values are listed in Table 2. Individual estimates of *B*_{obsd} were adjusted as described in Materials and Methods to obtain the corresponding values of *B*_{sp} plotted on the y-axis. The value of [*R*]_i used in the adjustment was taken as the mean of the individual values from the experiments represented in the analysis (A and B, 266 ± 72 pM, *N* = 7; C and D, 396 ± 57 pM, *N* = 6); the mean values of log [*P*]_i used for the adjustment in panels B and D are -7.44 ± 0.08 and -6.93 ± 0.09, respectively. Points shown at the lower end of the x-axis in panels B and D indicate binding in the absence of NMS.

assays. Both forms apparently can be activated by the addition of digitonin.

Temporary exposure to *N*-methylscopolamine was without effect on the capacity for [³H]quinuclidinylbenzilate in

cholate–NaCl, nor did it preclude the occurrence of latent sites. The data shown in Figure 3A are representative of four experiments in which receptors solubilized in cholate–NaCl were incubated transiently with *N*-methylscopolamine prior

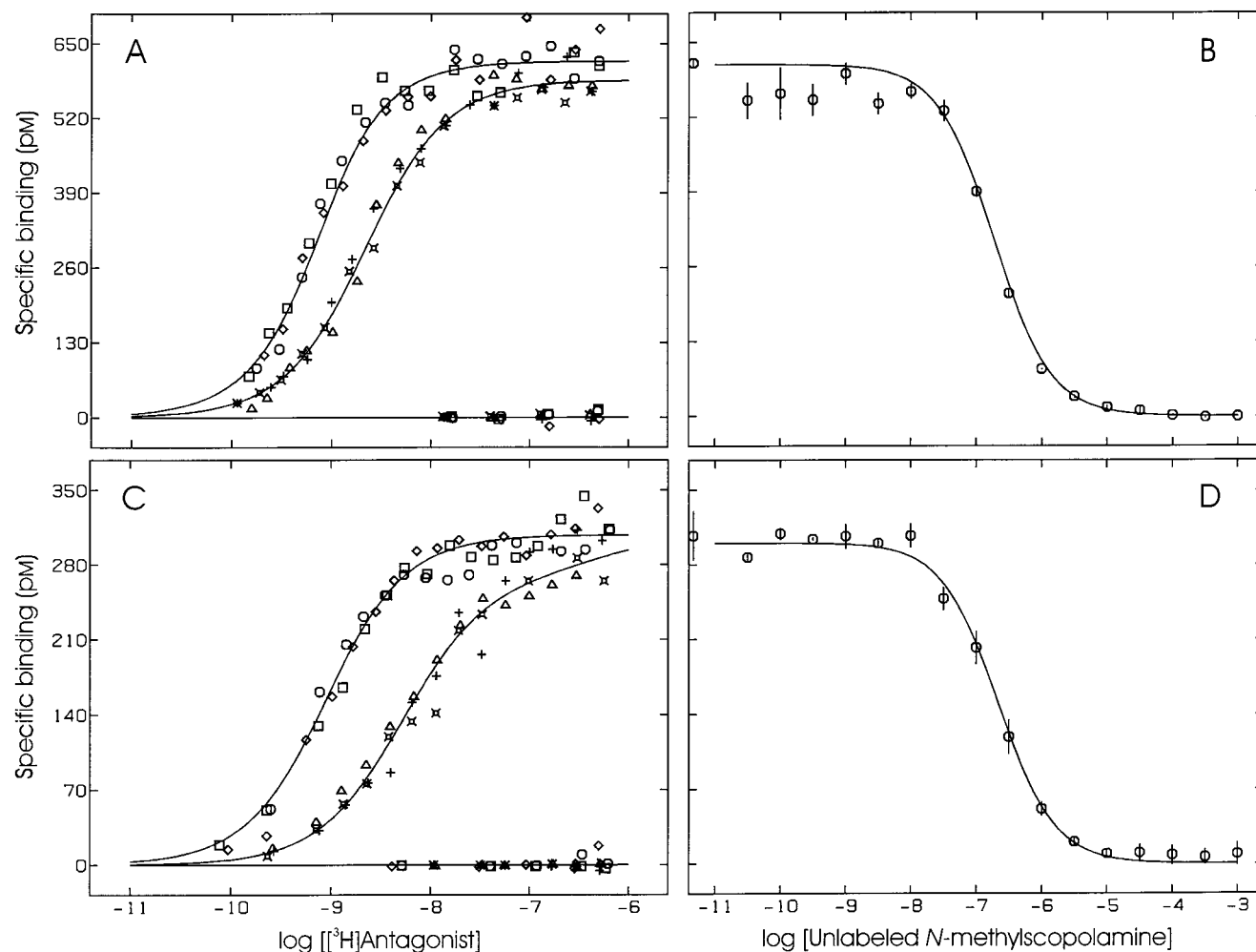


FIGURE 2: Binding to M_2 receptors in digitonin-cholate and in cholate-NaCl plus digitonin. Sarcolemmal membranes were solubilized in digitonin-cholate (A, B) or cholate-NaCl. The latter preparation was supplemented with digitonin following solubilization (C, D). (A, C) Total binding was measured at graded concentrations of $[^3\text{H}]\text{QNB}$ (\circ , \diamond , \square) and $[^3\text{H}]\text{NMS}$ (\triangle , ϕ , $+$), either alone (upper curves) or in the presence of 1 mM unlabeled NMS (baseline). The results from six independent experiments are shown (A, $N = 3$; C, $N = 3$). (B, D) Total binding was measured at a near-saturating concentration of $[^3\text{H}]\text{QNB}$ and graded concentrations of unlabeled NMS (B, $N = 3$; D, $N = 3$). The lines represent the best fits of eq 2 to the pooled data from all experiments represented in panels A and B ($N = 6$) or in panels C and D ($N = 6$). The parametric values are listed in Table 2. The mean values of $[R]_t$ used to obtain the adjusted values of B_{sp} are 619 ± 32 pM (A, B; $N = 6$) and 308 ± 55 pM (C, D; $N = 6$); the mean values of $\log [P]_t$ are -7.49 ± 0.01 (B) and -7.52 ± 0.13 (D). Further details are described in the legend to Figure 1.

to the binding assays. The concentration of *N*-methylscopolamine was chosen to be saturating according to the binding profile described by the radiolabeled analogue (i.e., $0.56 \mu\text{M}$). Both the capacity for $[^3\text{H}]\text{quinuclidinylbenzilate}$ and its affinity were essentially the same in the pretreated sample and in an untreated control. Since the capacity for $[^3\text{H}]\text{quinuclidinylbenzilate}$ was unaffected by *N*-methylscopolamine, the shortfall in capacity for *N*- $[^3\text{H}]\text{methylscopolamine}$ evident in Figure 1A was not associated with an irreversible change in the receptor. Similarly, transient incubation with *N*-methylscopolamine was without lasting effect on the recovery of latent receptors by digitonin, as indicated by the increased capacity for $[^3\text{H}]\text{quinuclidinylbenzilate}$ upon the addition of digitonin to the pretreated sample (Figure 3B).

No latency was observed with either *N*- $[^3\text{H}]\text{methylscopolamine}$ or $[^3\text{H}]\text{quinuclidinylbenzilate}$ when digitonin was added prior to the binding assay, either at the time of solubilization (Figure 2A) or after extraction in cholate-NaCl (Figure 2C). To examine the possibility that digitonin protects against an otherwise irreversible loss, receptor

solubilized in cholate-NaCl was incubated with each radioligand, and the time course of binding was monitored as illustrated in Figure 4. A stable level of binding was attained within about 60 min for $[^3\text{H}]\text{quinuclidinylbenzilate}$ and about 20 min for *N*- $[^3\text{H}]\text{methylscopolamine}$ at the near-saturating concentrations used in the experiment. A similar pattern was obtained for each radiolabeled antagonist with receptors solubilized in Lubrol-PX. Digitonin then was added after 120 or 45 min (Figure 4), and binding increased 1.3-fold for $[^3\text{H}]\text{quinuclidinylbenzilate}$ and 2.1-fold for *N*- $[^3\text{H}]\text{methylscopolamine}$. The relative levels of binding attained after equilibration in cholate-NaCl alone and after the addition of digitonin are commensurate with the relative capacities estimated from binding profiles at graded concentrations of each radioligand (e.g., Figures 1A and 2C). Thus, labeling by *N*- $[^3\text{H}]\text{methylscopolamine}$ was 63% of that by $[^3\text{H}]\text{quinuclidinylbenzilate}$ after the initial equilibration in the absence of digitonin (Figure 4); similarly, the convergence that followed the addition of digitonin is consistent with a relative capacity near 1. These results indicate that the latency

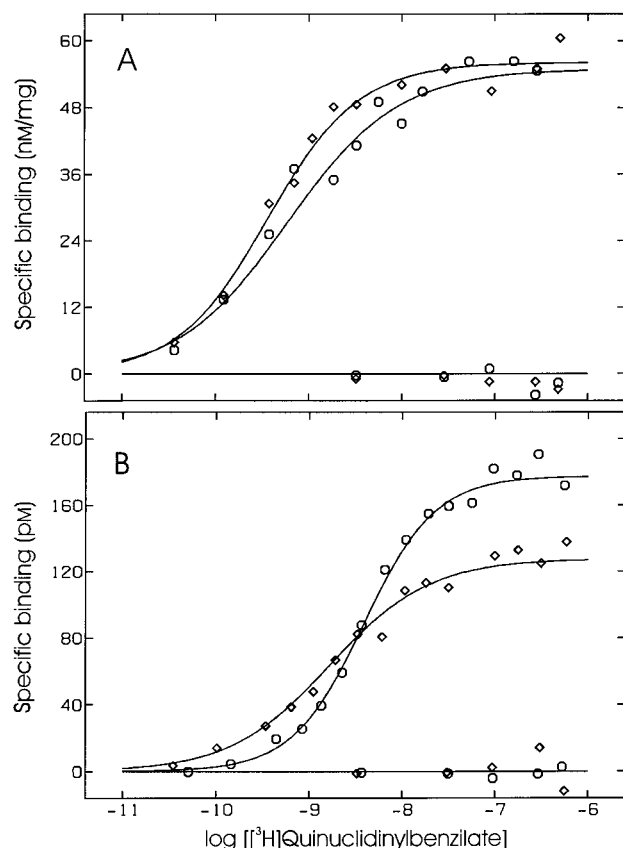


FIGURE 3: Recovery of latent sites from M_2 receptors solubilized in cholate-NaCl. Total binding was measured at graded concentrations of $[^3\text{H}]\text{QNB}$ either alone (upper curves) or in the presence of 1 mM unlabeled NMS (baseline). Data presented in the same panel were obtained in parallel. (A) Receptor solubilized in cholate-NaCl was incubated with a saturating concentration of unlabeled NMS (0.56 μM) for 45 min, and the ligand then was removed on a column of Sephadex G-50 (◇). Receptor that had not been incubated with ligand was processed on Sephadex G-50 and used as a control (○). The eluant was collected in each case and characterized for the binding of $[^3\text{H}]\text{QNB}$. (B) Receptor solubilized in cholate-NaCl was incubated with a saturating concentration of unlabeled NMS and processed on Sephadex G-50 as described above. The eluant was supplemented with digitonin (○) or with an equal volume of buffer (◇) and assayed for the binding of $[^3\text{H}]\text{QNB}$. The data in each panel are representative of four such experiments.

observed in cholate-NaCl is reversible for both $[^3\text{H}]\text{quinuclidinylbenzilate}$ and $N\text{-}[^3\text{H}]\text{methylscopolamine}$, since binding was regained when digitonin was added to receptors preequilibrated with either radioligand. The shortfall in capacity therefore was not a consequence of thermal denaturation or other instability after solubilization in cholate-NaCl.

The stability evident in the time dependence of binding at near-saturating levels of $N\text{-}[^3\text{H}]\text{methylscopolamine}$ was found at all concentrations of the radioligand. Receptors solubilized in cholate-NaCl were incubated with $N\text{-}[^3\text{H}]\text{methylscopolamine}$ for the usual period of 45 min and a longer period of 2 h, and the two binding profiles are superimposable (Figure 5).

Both radiolabeled antagonists are supplied as a solution in ethanol, and the final concentration of ethanol in assays containing $N\text{-}[^3\text{H}]\text{methylscopolamine}$ was 4–5% at the highest concentrations of the radioligand. Purified M_2 receptors have been found to be unstable under some

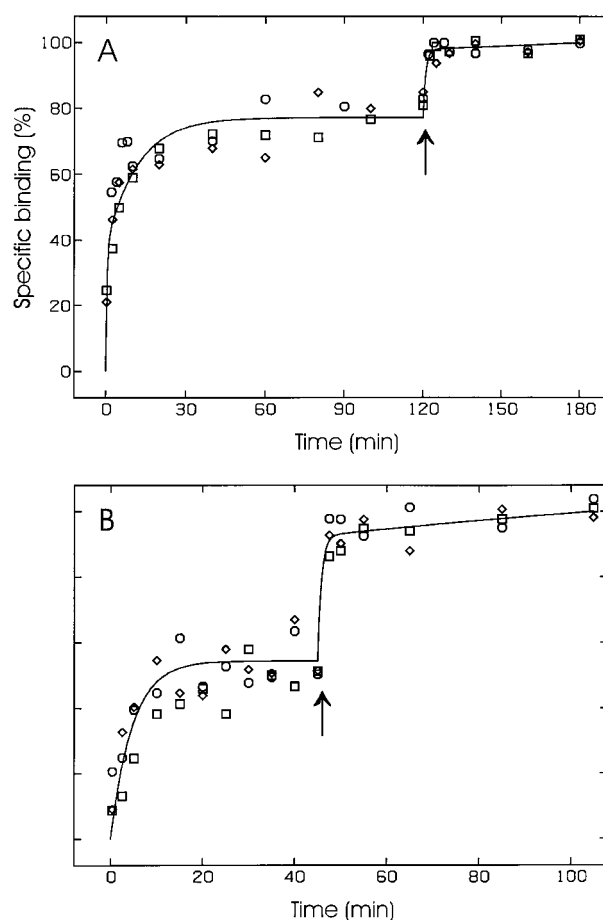


FIGURE 4: Time course for the binding of $[^3\text{H}]\text{quinuclidinylbenzilate}$ and $N\text{-}[^3\text{H}]\text{methylscopolamine}$ in cholate-NaCl. Receptor solubilized in cholate-NaCl was incubated at 30 °C with a saturating concentration of $[^3\text{H}]\text{QNB}$ (A, 13–36 nM) or $[^3\text{H}]\text{NMS}$ (B, 240–530 nM). At the time indicated by the arrow, the reaction mixture was supplemented with digitonin in buffer B to obtain a final concentration of 0.4%. Binding was assayed by means of aliquots (50 μL) removed from the reaction mixture at the times shown, and values obtained after the addition of digitonin were adjusted for the small reduction in the concentration of receptor (<5%). Data from three different experiments are represented in each panel (○, ◇, □), and each point represents the mean of two determinations. Nonspecific binding (B_{ns}) was estimated in parallel assays at the same concentration of $[^3\text{H}]\text{QNB}$ or $[^3\text{H}]\text{NMS}$. Maximal specific binding was defined as the mean of the last two points in each experiment, and the individual values at each time were normalized to that value taken as 100.

conditions, either in the absence of ligand or at any concentration of $N\text{-}[^3\text{H}]\text{methylscopolamine}$, when the reaction mixture contains ethanol at concentrations greater than about 1 vol %.³ In cholate-NaCl, however, there was no discernible difference in either the affinity or the capacity for $N\text{-}[^3\text{H}]\text{methylscopolamine}$ when the ethanol was evaporated to reduce its concentration in the reaction mixture to less than 1% (v/v).

$N\text{-}[^3\text{H}]\text{Methylscopolamine}$ dissociates rapidly from cardiac muscarinic receptors (e.g., ref 47), in contrast to the slow dissociation of $[^3\text{H}]\text{quinuclidinylbenzilate}$. The difference raises the possibility that the differential capacity observed in some detergents might be due, wholly or in part, to the selective dissociation of one radioligand on the columns of

³ Chi Shing Sum and James W. Wells, unpublished observations.

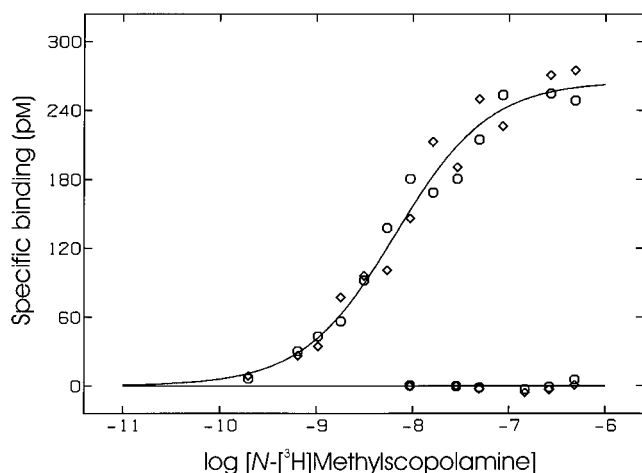


FIGURE 5: Stability in the binding of N -[^3H]methylscopolamine to receptor solubilized in cholate–NaCl. Total binding was measured at graded concentrations of [^3H]NMS, either alone (upper curves) or in the presence of 1 mM unlabeled NMS (baseline). The receptor was incubated with the radioligand at 30 °C for either 45 min (\circ) or 2 h (\diamond). The line represents the best fit of eq 1 with single values of EC_{50} , n_H , and B_{max} common to both sets of data, and the parametric values are as follows: $\log \text{EC}_{50} = -8.18 \pm 0.06$, $n_H = 0.89 \pm 0.08$, and $B_{\text{max}} = 265 \pm 11$ pM. There is no appreciable decrease in the sum of squares with separate rather than single values of EC_{50} , n_H , and B_{max} for the data obtained after 45 min and 2 h ($P = 0.20$). The results shown in the figure are representative of two experiments.

Sephadex G-50 used in the binding assays. To probe for this and other effects related to the separation of free and bound ligand, N -[^3H]methylscopolamine and [^3H]quinuclidinylbenzilate were equilibrated with sacrolemmal extracts in cholate–NaCl and monitored in the eluate from the column. Elution profiles from two columns are illustrated in Figure 6: one prepared at the standard length of 6.5 cm and a longer column of 8.0 cm. The length of the column had little or no effect on the area of the peak obtained with either radioligand, suggesting that the apparent capacity for N -[^3H]methylscopolamine is not reduced by leaching of the probe from the receptor. Also, each ligand was present at a near-saturating concentration, and the entire peak from the shorter column was contained in the volume of 1.45 mL collected in the binding assays. The relative area of 0.49 is consistent with the relative capacity estimated when the peak was collected in one fraction at multiple concentrations of each radioligand. In addition, there was no discernible difference in the relative capacity when the free and bound radioligands were separated at 4 °C rather than at room temperature.

Assessment of Differential Capacity in Terms of Scheme 1. If the system is at thermodynamic equilibrium, a difference in the apparent capacity for [^3H]quinuclidinylbenzilate and N -[^3H]methylscopolamine points to a subpopulation of sites inaccessible to the latter. Such a possibility was investigated further by examining the inhibitory effect of unlabeled N -methylscopolamine on the binding of [^3H]quinuclidinylbenzilate at near-saturating concentrations of the latter. Binding was measured after incubation of the reaction mixture for 2 h, and the data are illustrated in the right-hand panels of Figure 1. The time dependence of the reaction was examined in cholate–NaCl, and there was no appreciable difference in either the Hill coefficient or the inhibitory potency (IC_{50}) of N -methylscopolamine when the samples

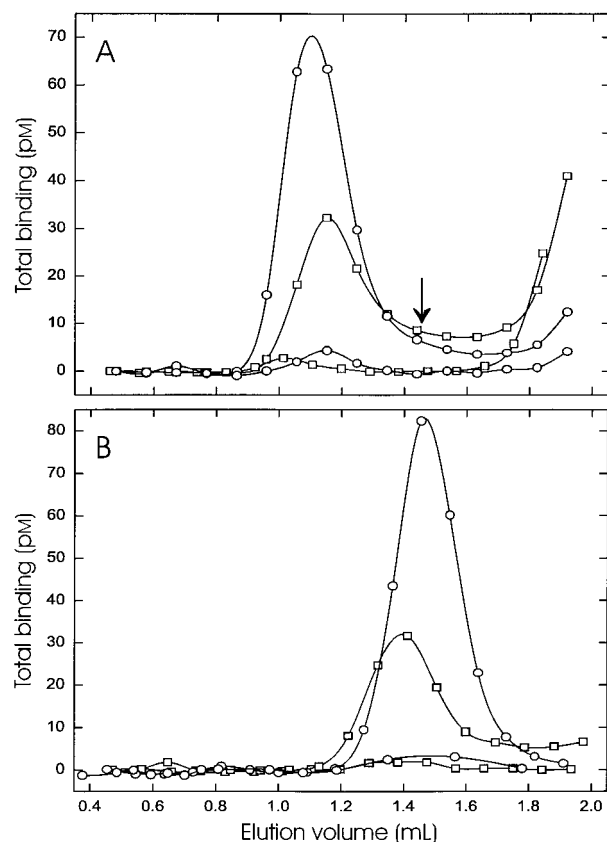


FIGURE 6: Separation of free and bound N -[^3H]methylscopolamine and [^3H]quinuclidinylbenzilate on Sephadex G-50. Receptor solubilized in cholate–NaCl was incubated with saturating concentrations of [^3H]NMS (\square , 145 nM) or [^3H]QNB (\circ , 174 nM), either alone (upper curves) or in the presence of 1 mM unlabeled NMS (baseline). An aliquot (50 μL) was applied to a column of Sephadex G-50 (A, 6.5 cm; B, 8.0 cm), and the eluate was monitored for radioactivity. The peaks visible in the figure emerged at the void volume and represent radioligand bound to the receptor. The free radioligand was retarded and eluted as a separate peak, the leading edge of which is visible in the case of the shorter column. The amounts of specifically bound radioligand in the void volume are as follows: 6.5 cm column (1.45 mL), 8.69 fmol of [^3H]NMS and 17.7 fmol of [^3H]QNB; 8.0 cm column (1.8 mL), 9.23 fmol of [^3H]NMS and 19.0 fmol of [^3H]QNB. Routine assays were performed with 6.5 cm columns, and the volume of the eluate collected for counting is indicated by the arrow.

were incubated for 4 or 6 h. Since complete or nearly complete inhibition was achieved at comparatively low concentrations of N -methylscopolamine, the unlabeled ligand appears to inhibit at sites to which the radiolabeled analogue cannot bind. Such an arrangement is inconsistent with the notion of distinct, independent, and noninterconvertible sites represented by Scheme 1.

The results of analyses in terms of Scheme 1 are summarized in Table 2 for each extract of receptor; the corresponding sums of squares are listed in Table 3, and the fitted curves are shown by the lines in Figures 1 and 2. Each analysis was arranged such that all of the data represented in the left- and right-hand panels of Figures 1 and 2 shared a common value of F_2 , in accord with the presumption that there is no interconversion among the different states or forms of the receptor. Similarly, the affinity of quinuclidinylbenzilate for each state was estimated as the single value of K_{Pj} common to all data acquired with [^3H]quinuclidinylbenzilate as the radioligand. In contrast, the affinity of

Table 2: Affinities of Quinuclidinylbenzilate and *N*-Methylscopolamine Estimated Empirically in Terms of Scheme 1^a

solubilized preparation	L	quinuclidinylbenzilate		<i>N</i> -methylscopolamine		F_2^b
		log K_{P1}	log K_{P2}	log K_{L1}	log K_{L2}	
cholate—NaCl	P (3)	−9.97 ± 0.12	−9.11 ± 0.11	−8.47 ± 0.06	−5.45 ± 0.28 ^c	0.49 ± 0.02
	A (4)			−9.22 ± 0.14	−7.34 ± 0.13	
Lubrol-PX	P (3)	−7.87 ± 0.11	−7.54 ± 0.21	−7.15 ± 0.05	> −5.8 ^d	0.44 ± 0.04
	A (3)			−7.41 ± 0.13	−6.48 ± 0.22	
digitonin—cholate	P (3)	−9.38 ± 0.03 ^e	−9.38 ± 0.03 ^e	−8.72 ± 0.02	> −6.7 ^d	0.05 ± 0.01
	A (3)			−8.61 ± 0.04 ^f	−8.61 ± 0.04 ^f	
cholate—NaCl + digitonin	P (3)	−9.13 ± 0.03 ^g	−9.13 ± 0.03 ^g	−8.29 ± 0.03	−6.28 ± 0.49 ^c	0.12 ± 0.03
	A (3)			−8.28 ± 0.05 ^h	−8.28 ± 0.05 ^h	

^a The data illustrated in the paired left- and right-hand panels of Figures 1 and 2 were analyzed according to eq 2 ($n = 2$) to obtain the fitted curves shown in the figure and the parametric values listed in the table. QNB was present only as the radioligand ($L \equiv P$, both panels of Figures 1 and 2), while NMS was present as either the radioligand ($L \equiv P$, left-hand panels) or the unlabeled analogue ($L \equiv A$, right-hand panels). The number of experiments is shown in parentheses. For QNB, single values of K_{Pj} were common to all of the data shown in the right-hand panel and to those data acquired at graded concentrations of [³H]QNB in the left-hand panel; for [³H]NMS, single values of K_{Aj} were common to all of the data shown in the right-hand panel, and single values of K_{Pj} were common to those data acquired at graded concentrations of [³H]NMS in the left-hand panel. A single value of F_2 was common to all of the data shown in both panels. Single values of $[R]_i$ were common to all data acquired within the same experiment, and single values of NS were common to data acquired with the same radioligand in the same experiment. Differences in the fitted values of K_{Pj} and K_{Aj} for NMS constitute a discrepancy between the model and the data. ^b The fraction of sites exhibiting low affinity for [³H]NMS. The quantity $1 - F_2$ approximates the relative capacity of the preparation for [³H]NMS and [³H]QNB (cf. Table 1). ^c The value exceeds the highest concentration of the radioligand but is defined by a shallow minimum in the weighted sum of squares. ^d The value of K_{P2} for [³H]NMS is essentially undefined, and the parameter therefore was mapped to obtain the lower bound as identified by a significant increase in the weighted sum of squares ($P < 0.05$). At higher values of K_{P2} , the parameter is without effect on the sum of squares or on the values of other parameters; the latter were evaluated with the value of K_{P2} for [³H]NMS set at 0.1 M. ^{e–h} The parameters are indistinguishable and therefore were optimized as a single value.

Table 3: Comparison of Mechanistic Schemes for Binding to Solubilized Receptors^a

model	conditions for NMS	maximal labeling in cooperative systems		sum of squares			
		[³ H]QNB	[³ H]NMS	cholate— NaCl	Lubrol- PX	digitonin— cholate	cholate—NaCl + digitonin
multiple classes of sites (Scheme 1)							
empirical	$K_{Pj} \neq K_{Aj}$			6660	6549	10560	9948
mechanistically consistent	$K_{Pj} = K_{Aj}$			25180 ^b	11420 ^b	10870	11290
cooperativity (Scheme 2 and similar models)							
divalent receptor	$K_P = K_A$, $p_j = a_j$	2 sites ($p_j \sim 1$)	1 site ($a_2 > 10$)	19960	11060	<i>c</i>	<i>c</i>
trivalent receptor	$K_P = K_A$, $p_j = a_j$	2 sites ($p_2 \sim 1, p_3 > 10$)	1 site ($a_2 > 10$)	19460	11240	<i>c</i>	<i>c</i>
tetravalent receptor ^d	$K_P = K_A$, $p_j = a_j$	2 sites ($p_2 \sim 1, p_3 > 10$)	1 site ($a_2 > 10$)	18210	11080	<i>c</i>	<i>c</i>
tetravalent receptor ^d	$K_P = K_A$, $p_j = a_j$	4 sites ($p_j \sim 1$)	2 sites ($a_2 \sim 1, a_3 > 10$)	10120 ^e	6692 ^e	10210 ^{f,g}	9638 ^f
hexavalent receptor	$K_P = K_A$, $p_j = a_j$	6 sites ($p_j \sim 1$)	3 sites ($a_2, a_3 \sim 1, a_4 > 10$)	8657	6368	<i>c</i>	<i>c</i>
octavalent receptor	$K_P = K_A$, $p_j = a_j$	4 sites (p_2 – $p_4 \sim 1, p_5 > 10$)	2 sites ($a_2 \sim 1, a_3 > 10$)	8518	6582	<i>c</i>	<i>c</i>
octavalent receptor	$K_P = K_A$, $p_j = a_j$	8 sites ($p_j \sim 1$)	4 sites (a_2 – $a_4 \sim 1, a_5 > 10$)	7563	6336	<i>c</i>	<i>c</i>

^a The data illustrated in Figures 1 and 2 were analyzed according to Scheme 1 ($n = 2$) and various cooperative schemes. The constraints imposed in each analysis and the sum of squares obtained from each fit are listed in the table. In the case of Scheme 1, the analysis was performed both empirically and in a mechanistically consistent manner. In the empirical analysis, the dissociation constant of NMS was estimated separately for the radioligand and the unlabeled analogue; otherwise, a single value was common to both forms of the ligand. In the case of cooperative schemes, all parameters were assigned to enforce mechanistic consistency. The values of p_j and a_j were fixed as required to establish the apparent capacity of [³H]QNB relative to the true capacity ($n[R]_i$) and to ensure that the relative apparent capacity for [³H]NMS and [³H]QNB was consistent with the data. ^b With three classes of sites (Scheme 1, $n = 3$), the sum of squares is 19640 and 9517 for binding in cholate—NaCl and Lubrol-PX, respectively. ^c Not analyzed. ^d Scheme 2. ^e The results of these analyses are illustrated in Figure 8. ^f [³H]NMS was assumed to label all sites at the highest concentrations used in the experiments (i.e., $a_2 - a_4 \sim 1$). ^g The fit was achieved with no constraint on a_j , p_j , or c_j , which are highly correlated. There is no appreciable increase in the sum of squares (10270) if the values of c_j are fixed at 1, thereby precluding noncompetitive interactions between QNB and NMS; the corresponding values of p_j and a_j generally are near 1.

N-methylscopolamine for each state was estimated as two parameters: a value of K_{Pj} derived from the binding of *N*-[³H]-methylscopolamine alone (left-hand panel) and a value of K_{Aj} derived from the inhibitory effect on [³H]quinuclidinylbenzilate (right-hand panel). Since the labeled and unlabeled analogues of *N*-methylscopolamine are expected to be func-

tionally identical, any difference in the corresponding values of K_{Pj} and K_{Aj} constitutes a discrepancy between the model and the data. The values of F_2 listed in Table 2 indicate the fraction of sites inaccessible to *N*-[³H]methylscopolamine.

Owing to the differences in apparent capacity, two classes of sites are required to describe the system in cholate—NaCl

and Lubrol-PX: one class that binds both radioligands and a second that exhibits anomalously low affinity for N -[^3H]-methylscopolamine. The affinity of N -[^3H]-methylscopolamine for the sites labeled only by [^3H]quinuclidinylbenzilate in Lubrol-PX is essentially undefined, and the value of K_{P2} shown in Table 2 is the lower bound consistent with the data. Neither preparation required more than two classes of sites ($P > 0.05$).

The affinities listed for N -methylscopolamine in Table 2 highlight the discrepancy between its binding as measured directly and as inferred from its inhibitory effect on the binding of [^3H]quinuclidinylbenzilate. In cholate–NaCl, the sites inaccessible to N -[^3H]-methylscopolamine imply a value of K_{P2} that exceeds the highest concentration of radioligand used in the assays and is at least 70-fold greater than the value of K_{A2} inferred from the inhibition of [^3H]quinuclidinylbenzilate. A similar if somewhat smaller discrepancy is seen between the values of K_{P2} and K_{A2} for receptors solubilized in Lubrol-PX. Smaller discrepancies also emerge at the sites labeled by both radioligands, where the value of K_{P1} defined by graded concentrations of the radioligand exceeds the corresponding value of K_{A1} defined by the inhibitory effect on [^3H]quinuclidinylbenzilate.

To confirm these anomalies in the binding of N -methylscopolamine, the analyses summarized in Table 2 were repeated with the parameters assigned strictly in accord with the model. Thus, the affinity of N -methylscopolamine at each class of sites was assumed to be the same for binding of the radioligand alone and for the inhibition of [^3H]quinuclidinylbenzilate (i.e., $K_{Pj} = K_{Aj}$). This constraint was accompanied in each case by an increase of 1.7-fold or more in the sum of squares (Table 3, $P < 0.00001$). The constrained fit was improved when the degree of heterogeneity was increased from two classes of sites to three ($P < 0.05$), but it remained unsatisfactory relative to the fit obtained in the corresponding empirical analysis (i.e., $K_{Pj} \neq K_{Aj}$, $n = 3$, $P < 0.00001$). There was no further improvement in the sum of squares with four or more classes of sites ($P > 0.05$). It follows that Scheme 1 is inconsistent with the data regardless of the degree of heterogeneity assumed for the receptor.

A different pattern emerged for receptors solubilized in digitonin–cholate or in cholate–NaCl supplemented later with digitonin, where the relative capacity for N -[^3H]-methylscopolamine and [^3H]quinuclidinylbenzilate was near or equal to 1 (Table 1). In those preparations, comparatively small differences in capacity can lead to discrepant values of K_{P2} and K_{A2} for N -methylscopolamine at a minor fraction of the sites labeled by [^3H]quinuclidinylbenzilate (Table 2). The shortfall represented only 5% of all sites in digitonin–cholate, however, and the effect on the sum of squares was negligible when the values of K_{Pj} and K_{Aj} were assumed to be equal (Table 3, $P = 0.13$). Scheme 1 therefore is consistent with the data obtained under those conditions, and binding appears to be fully competitive. The shortfall in capacity represented 12% of all sites in cholate–NaCl plus digitonin, and the corresponding difference between K_{Pj} and K_{Aj} for N -methylscopolamine is significant (Table 3, $P = 0.00009$). Since the difference in capacity was about 50% in cholate–NaCl, the residual difference after the addition of digitonin may represent the incomplete recovery of sites from the latent or low-affinity state. Also, both preparations

may undergo a small loss of bound N -[^3H]-methylscopolamine on Sephadex G-50 in the binding assays.

It has been noted previously that nonradiolabeled contaminants present with the radioligand can reduce the estimates of both $[R]_t$ and K_P by a factor that depends on the amount of the impurity and the relative affinity of the two ligands for the receptor.⁴ Moreover, past batches of N -[^3H]-methylscopolamine have contained the synthetic precursor scopolamine in quantities sufficient to reduce B_{max} to about 75% of that found with [^3H]quinuclidinylbenzilate (48). The relative inhibitory potency of N -methylscopolamine and scopolamine was 0.16 ± 0.04 ($N = 4$) in cholate–NaCl.⁵ An excess of scopolamine over N -[^3H]-methylscopolamine therefore is required if the differential capacity in cholate–NaCl is to be described in terms of Scheme 1. The lines in Figure 7 represent the best fit of Scheme 1, formulated to accommodate an unlabeled contaminant (48). To describe the data represented in Figure 7A, the model requires a value of at least 3.7 for the ratio of scopolamine to N -[^3H]-methylscopolamine in that batch of the radioligand. In contrast, scopolamine was not detectable in the mass spectra of N -[^3H]-methylscopolamine used in the present investigation. Also, the differential capacity increased from about 0.5 in cholate–NaCl to about 0.9 upon the addition of digitonin. The same batch of N -[^3H]-methylscopolamine was used throughout, however, and the relative inhibitory potency was essentially unchanged at 0.11 ± 0.02 ($N = 3$).

The mass spectra obtained for N -[^3H]-methylscopolamine indicated the presence of triethylamine, which is used to elute the radioligand during purification on HPLC. Quaternary ammonium compounds are known to be muscarinic antagonists (49). In assays with [^3H]quinuclidinylbenzilate, however, the value of the K_A for triethylamine was found to exceed 0.1 mM in cholate–NaCl and in cholate–NaCl plus digitonin (Scheme 1, $n = 1$). Since the molar ratio of triethylamine to N -methylscopolamine never exceeded 0.70 in the mass spectrum, it is not expected to have an appreciable effect on the binding parameters of the radioligand.

To examine the possibility that a racemic mixture of (–)- and (+)-[^3H]quinuclidinylbenzilate contributed to the increase in capacity observed upon the addition of digitonin to receptors solubilized in cholate–NaCl, the affinities of the two enantiomers were compared in assays with [^3H]quinuclidinylbenzilate. The (–)-enantiomer was 403-fold more potent than the (+)-enantiomer in cholate–NaCl and 595-fold more potent in cholate–NaCl plus digitonin. It therefore seems unlikely that the latent sites revealed by

⁴ In terms of Scheme 1 ($n = 1$), the apparent values of both the capacity ($[R]_{t,\text{app}}$) and the dissociation constant of the radioligand ($K_{P1,\text{app}}$) are reduced by the factor $(1 + f_A K_P / K_A)$, where f_A represents the molar ratio of unlabeled contaminant to radioligand (i.e., $f_A = [A]/[P]_t$) (48). It is assumed here that the estimates of $[R]_{t,\text{app}}$ and $K_{P1,\text{app}}$ are based on the specific radioactivity stated by the manufacturer, which accounts only for the relative amounts of stable and unstable isotope in that batch of radioligand (e.g., ^1H and ^3H).

⁵ The relative inhibitory potencies stated in the text for NMS and scopolamine ($\text{IC}_{50,\text{NMS}}/\text{IC}_{50,\text{SCO}}$) are the means ($\pm \text{SEM}$) of individual values estimated from assays that included both unlabeled antagonists taken in parallel (cf. Figure 7B). The data were analyzed according to the equation $B_{\text{obsd}} = (B_{[L]=0} - B_{[L] \rightarrow \infty}) \{ \text{IC}_{50}^{n_H} / (\text{IC}_{50}^{n_H} + [L]^{n_H}) \} + B_{[L] \rightarrow \infty}$, and the mean values of n_H for NMS and scopolamine are as follows: in cholate–NaCl, 0.91 ± 0.10 and 1.30 ± 0.08 ($N = 4$); in cholate–NaCl plus digitonin, 0.79 ± 0.02 and 1.15 ± 0.04 ($N = 3$).

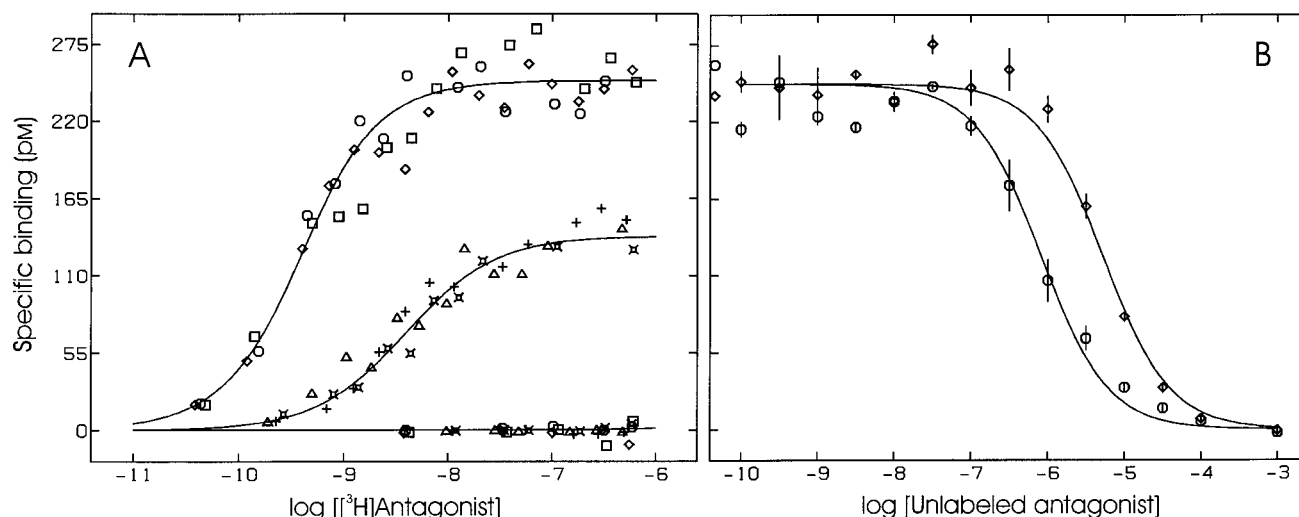


FIGURE 7: Estimation of the level of scopolamine required to reconcile the discrepancies between Scheme 1 and the binding properties of M_2 receptors solubilized in cholate-NaCl. (A) The data are the same as those shown in Figure 1A. (B) Total binding was measured at a saturating concentration of $[^3\text{H}]\text{QNB}$ and graded concentrations of unlabeled NMS (\circ) or scopolamine (\diamond). Each experiment included assays with both unlabeled antagonists, taken in parallel, and the results of three separate experiments are represented in the figure. The lines illustrate the best fit of Scheme 1 ($n = 1$) to the data represented in both panels taken together. The model was formulated as described previously (i.e., eqs 3 and 4 in ref 48), with scopolamine, NMS, and QNB designated as ligands 1, 2, and 3, respectively. The total concentration of scopolamine necessary to account for the differential capacity for $[^3\text{H}]\text{NMS}$ and $[^3\text{H}]\text{QNB}$ in panel A was estimated relative to that of $[^3\text{H}]\text{NMS}$ (i.e., $f_1 = [L_1]/[L_2]_t$). Single values of $[R]_t$ were common to all data from the same experiment, and a single value of f_1 was common to all of the data obtained at graded concentrations of $[^3\text{H}]\text{NMS}$. The fitted value of f_1 is 5.1 ± 0.7 , and the estimates of affinity are as follows: $\log K_{11} = -7.36 \pm 0.05$ (scopolamine), $\log K_{21} = -8.16 \pm 0.04$ (NMS), and $\log K_{31} = -9.57 \pm 0.04$ (QNB). Individual estimates of B_{obsd} were normalized to the mean value of $[R]_t$ for all of the data included in the analysis (i.e., $[R]_t = 249 \pm 25$ pM, $N = 6$), and the corresponding value of B_{sp} is plotted on the y-axis. The mean value of $\log [L_3]$ for the adjustment in panel B is -7.49 ± 0.01 .

digitonin were due to an optically impure radioligand. Moreover, since both forms of $[^3\text{H}]\text{quinuclidinylbenzilate}$ are expected to be tritiated, a racemate is not expected to yield spurious estimates of B_{max} .⁶

Assessment of Differential Capacity in Terms of Scheme 2. The possibility of cooperative interactions was examined in terms of Scheme 2, in which the low relative capacity for N - $[^3\text{H}]\text{methylscopolamine}$ in cholate-NaCl and Lubrol-PX can be attributed to a high degree of negative cooperativity between two successive equivalents of the radioligand. If the value of p_j is sufficiently large, the macroscopic dissociation constant for the j th equivalent of N - $[^3\text{H}]\text{methylscopolamine}$ will exceed the highest concentration used in the assays (i.e., $\{j/(n - j + 1)\} \prod_{i=2}^j p_i K_P \gg [P]_{\text{max}}$). Binding therefore will be precluded, both to the j th site and to additional sites provided that the effect of p_j is not offset by small values of p_{j+k} ($j < k \leq n$). The inhibitory effect of N -methylscopolamine will derive in part from competition for the vacant receptor and in part from cooperativity between the unlabeled ligand and $[^3\text{H}]\text{quinuclidinylbenzilate}$. The latter route is represented in Scheme 2 by those states that include the receptor and both ligands.

⁶ When the radiolabeled probe is a racemate (i.e., $P_{(-)}$ and $P_{(+)}$), total specific binding to identical and mutually independent sites (R) in a system at equilibrium is described by a rectangular hyperbola as follows: $B_{\text{sp}} = [P_{(-)}R] + [P_{(+)}R] \equiv [R]_t[P]/(K_{\text{app}} + [P])$, where $[R]_t = [R] + [P_{(-)}R] + [P_{(+)}R]$, $[P] = [P_{(-)}] + [P_{(+)}]$, $K_{\text{app}} = K_{(-)}K_{(+)} / (f_{(-)}K_{(+)} + f_{(+)}K_{(-)})$, $f_{(\pm)} = [P_{(\pm)}]/[P]$ (i.e., $f_{(-)} + f_{(+)} = 1$), and $K_{(\pm)} = [P_{(\pm)}][R]/[P_{(\pm)}R]$. The estimate of capacity, therefore, is independent of the racemic nature of the radioligand (i.e., $B_{\text{max}} = [R]_t$). The quantities $[P_{(-)}]$ and $[P_{(+)}]$ denote the free concentrations of the two enantiomers, which are assumed here to equal the total concentrations. While some depletion may occur at lower concentrations of ligand, it will become negligible as the receptor becomes saturated.

Scheme 2 provides a good approximation of the binding properties of receptors extracted in cholate-NaCl or Lubrol-PX, as illustrated by the fitted curves in Figure 8. The corresponding parametric values are listed in the accompanying legend. Some parameters are highly correlated or otherwise undefined by the present data, and those values were fixed within acceptable bounds identified by mapping. All parameters were assigned to enforce mechanistic consistency. The model therefore can account both for the binding of N - $[^3\text{H}]\text{methylscopolamine}$ and for the inhibitory effect of unlabeled N -methylscopolamine, in contrast to the inconsistencies that emerge from analyses in terms of Scheme 1.

The apparent capacity for N - $[^3\text{H}]\text{methylscopolamine}$ was about 50% of that for $[^3\text{H}]\text{quinuclidinylbenzilate}$ in both detergents (Table 1). It was assumed in each analysis that there was little or no cooperativity in the binding of $[^3\text{H}]\text{quinuclidinylbenzilate}$ (i.e., $0.1 < p_j < 10$), which therefore labeled all sites of the tetravalent receptor under the conditions of the assays. Under those circumstances, the maximal binding of N - $[^3\text{H}]\text{methylscopolamine}$ is the result of little or no cooperativity between the first and second equivalents (i.e., $\log a_2 = 0.2$ or -0.2) and strong negative cooperativity between the second and third equivalents (i.e., $\log a_3 > 1$). The inhibitory effect of unlabeled N -methylscopolamine at the sites labeled only by $[^3\text{H}]\text{quinuclidinylbenzilate}$ is a consequence of cooperative interactions between the two ligands (i.e., $c_j \neq 1$), and an acceptable fit cannot be achieved if the analysis is constrained to prohibit such effects (i.e., $c_j = 1$).

The results illustrated in Figure 8 are based on the assumption of a tetravalent receptor in which all of the sites are accessible to $[^3\text{H}]\text{quinuclidinylbenzilate}$. This turns out

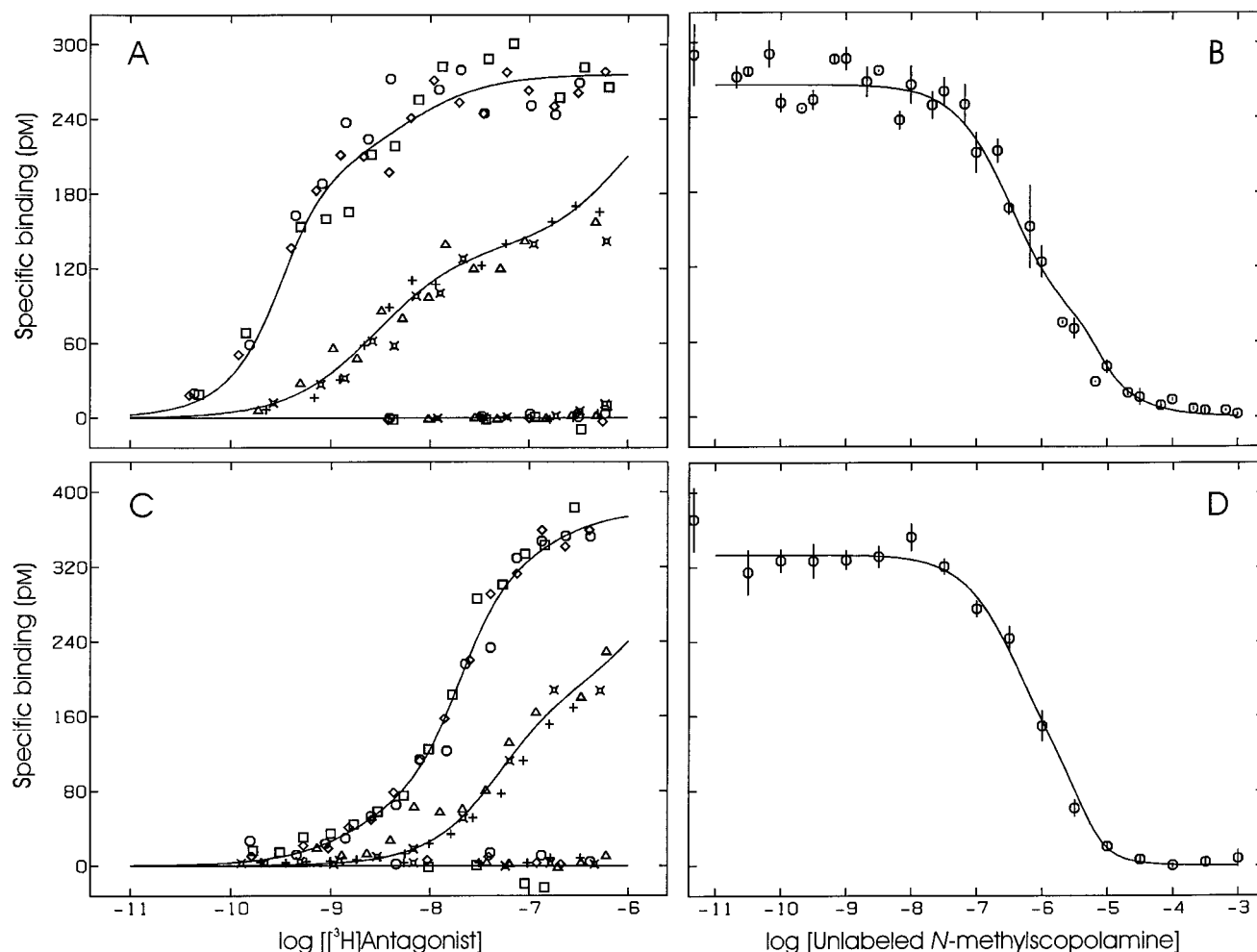


FIGURE 8: Binding to M_2 receptors solubilized in cholate-NaCl and Lubrol-PX, described in terms of Scheme 2. Sarcolemmal membranes were solubilized in cholate-NaCl (A, B) or Lubrol-PX (C, D). (A, C) Total binding was measured at graded concentrations of $[^3\text{H}]\text{QNB}$ (\circ , \diamond , \square) and $[^3\text{H}]\text{NMS}$ (Δ , \diamond , $+$), either alone (upper curves) or in the presence of 1 mM unlabeled NMS (baseline). (B, D) Total binding was measured at a near-saturating concentration of $[^3\text{H}]\text{QNB}$ and graded concentrations of unlabeled NMS. The data are the same as those shown in Figure 1. The lines represent the best fits of eq 3c (i.e., eq 3, $n = 4$) to the pooled data from the seven experiments represented in panels A and B and, in a separate analysis, to the pooled data from the six experiments represented in panels C and D. $[^3\text{H}]\text{QNB}$ was taken as ligand P, and both $[^3\text{H}]\text{NMS}$ and unlabeled NMS were taken throughout as ligand A. All parameters were assigned to enforce mechanistic consistency, and single values of K_P , K_A , p_j , a_j , and c_j therefore were common to all of the relevant data. Data acquired at graded concentrations of $[^3\text{H}]\text{QNB}$ are irrelevant to K_A , a_j , and c_j ; similarly, those at graded concentrations of $[^3\text{H}]\text{NMS}$ are irrelevant to K_P , p_j , and c_j . Single values of $[R]_t$ were common to all data acquired within the same experiment. The fitted values for binding in cholate-NaCl (A, B) are as follows: $\log K_P = -9.08 \pm 0.10$, $\log p_2 = -0.60 \pm 0.16$, $\log p_4 = 0.87 \pm 0.21$, $\log K_A = -8.26 \pm 0.08$, $\log a_2 = 0.20 \pm 0.18$, $\log a_3 = 1.63 \pm 0.16$, $\log c_2 = -3.04 \pm 0.24$, $\log c_3 = 8.93 \pm 5.53$, and $\log c_4 = -4.96 \pm 4.98$. The values of $\log p_2$ and $\log p_3$ are highly correlated, and the latter was fixed at zero to stabilize the convergence. The value of $\log a_4$ is essentially undefined and was fixed arbitrarily at zero. The values of $\log c'_3$, $\log c'_4$, and $\log c''_4$ are incompletely defined by the data and were fixed at 8. The fitted values for binding in Lubrol-PX (C, D) are $\log K_P = -7.95 \pm 0.07$, $\log p_2 = 0.80 \pm 0.44$, $\log p_3 = -1.12 \pm 0.83$, $\log p_4 = 0.63 \pm 0.73$, $\log K_A = -6.83 \pm 0.06$, $\log a_2 = -0.19 \pm 0.16$, $\log c_2 = -1.01 \pm 0.19$, $\log c_3 = \log c'_3 = 1.98 \pm 0.38$. The values of $\log c_4$, $\log c'_4$, and $\log c''_4$ are incompletely defined and were fixed at 0.7, as determined by mapping. The value of $\log a_3$ was fixed at 1, as determined by mapping; that of $\log a_4$ was essentially undefined and fixed at zero. The mean values of $[R]_t$ used to obtain the adjusted values of B_{sp} are 69 ± 19 pM (A, B; $N = 7$) and 95 ± 14 pM (C, D; $N = 6$). Further details are described in the legend to Figure 1.

to be the simplest cooperative arrangement consistent with the data, the occurrence of undefined parameters notwithstanding. Various other possibilities are listed in Table 3, together with the corresponding sums of squares for the data represented in Figure 8. The only restriction was the requirement that the apparent capacity for N - $[^3\text{H}]\text{methylscopolamine}$ be 50% of that for $[^3\text{H}]\text{quinuclidinylbenzilate}$. Consistency with the data can be assessed with reference to Scheme 1, where the excellent but empirical fit illustrates what might be expected of the true model; the poor but mechanistically consistent fit represents the minimal level of agreement to be expected of any alternative to Scheme 1.

The values listed in Table 3 indicate that a tetravalent receptor in which two of the four sites are accessible to N - $[^3\text{H}]\text{methylscopolamine}$ can provide a fit comparable to that obtained empirically in terms of Scheme 1. While the di- and trivalent alternatives can describe the binding of the radioligands alone, neither can reconcile the behavior of labeled and unlabeled N -methylscopolamine. Moreover, the increase in the apparent capacity for $[^3\text{H}]\text{quinuclidinylbenzilate}$ when extracts in cholate-NaCl are supplemented with digitonin suggests that up to 50% of the sites can be latent for that radioligand. If that latency derives from negative cooperativity, a tetramer is no longer sufficient to describe

the data; rather, at least six and perhaps as many as eight interacting sites are required, suggesting that the receptor is larger than a tetramer.

With receptor extracted in digitonin–cholate, a mechanistically consistent fit is possible with Scheme 1, as described above (Table 3). An essentially equivalent fit is obtained in terms of Scheme 2, in which the competitive behavior and similar capacities derive from values near 1 for the cooperativity factors p_j , a_j , and particularly c_j (Table 3). The detergent therefore appears to regulate cooperativity within the receptor, and cooperative effects are largely absent from extracts in digitonin–cholate.

DISCUSSION

Muscarinic receptors can exhibit a striking heterogeneity toward antagonists in detergent-solubilized extracts from porcine atria. Since the apparent capacity for N -[^3H]methylscopolamine was only about 50% of that for [^3H]quinuclidinylbenzilate in cholate–NaCl and Lubrol-PX, a large subpopulation of sites appears to be of anomalously weak affinity for N -methylscopolamine under those conditions. No such anomaly occurred with extracts in digitonin–cholate, where the capacity for N -[^3H]methylscopolamine and [^3H]quinuclidinylbenzilate was essentially the same.

Sites that apparently were latent with respect to N -[^3H]methylscopolamine were recovered when digitonin was added to preparations extracted in cholate–NaCl. Moreover, supplementary digitonin not only eliminated the difference in capacity between N -[^3H]methylscopolamine and [^3H]quinuclidinylbenzilate but also increased the absolute capacity for both radioligands. Latency therefore is not unique to N -[^3H]methylscopolamine, and it may be that no radioligand can bind to all of the receptors with characteristic muscarinic affinity under some conditions. This introduces a degree of uncertainty as to the true capacity under any condition.

A shortfall in the maximal binding of N -[^3H]methylscopolamine has been noted previously in a variety of circumstances (see ref 48 and references cited therein). The effect typically has been rationalized in terms of Scheme 1 per se or formally equivalent models. The higher capacity for [^3H]quinuclidinylbenzilate often is attributed to its lipophilicity, which would allow selective access to sites localized behind a hydrophobic barrier. Also, N -[^3H]methylscopolamine might differentiate among distinct and non-interconverting forms of the receptor, perhaps arising from differences in posttranslational processing or representing different subtypes. Neither possibility can account for the present data, however, owing to the inability of Scheme 1 to reconcile the binding of N -[^3H]methylscopolamine with the inhibitory effect of unlabeled N -methylscopolamine on the binding of [^3H]quinuclidinylbenzilate. The possibility of multiple isoforms also is precluded by the evidence that muscarinic receptors from porcine atria are wholly or predominantly of the M_2 subtype (50, 51).

Binding of N -[^3H]methylscopolamine and [^3H]quinuclidinylbenzilate to cholate–NaCl-solubilized receptors attained a maximum and thereafter was independent of time (Figures 4 and 5). Also, the binding of [^3H]quinuclidinylbenzilate was not affected by transient incubation of the receptors with N -methylscopolamine. Both the absolute and the relative capacities for N -[^3H]methylscopolamine were increased when

extracts in cholate–NaCl were supplemented with digitonin either before or after incubation with the radioligand. It therefore appears that the system was at equilibrium in the binding assays, that there were no irreversible effects, and that the different states of affinity implied by a differential capacity and latent sites are interconvertible. The failure of Scheme 1 highlights the noncompetitive nature of the interaction between [^3H]quinuclidinylbenzilate and N -methylscopolamine, which appears to inhibit at sites to which it cannot bind. It follows that the multiple states of affinity revealed by the two radioligands may derive from induced heterogeneity caused, either directly or indirectly, by clustering of the sites in oligomeric arrays.

Within an oligomeric cluster, a difference in the apparent capacity for N -[^3H]methylscopolamine and [^3H]quinuclidinylbenzilate could arise from cooperative effects, asymmetry, or a combination of the two. If the system is strictly cooperative (e.g., Scheme 2), full occupancy is precluded by a high degree of negative cooperativity between two successive equivalents of antagonist (i.e., $p_j > 10$); that is, the macroscopic dissociation constant for the j th equivalent of the radioligand exceeds the highest concentration used. Since each complex is functionally symmetric, the microscopic affinity is the same for all vacant sites at less than full occupancy. If the system is strictly asymmetric [e.g., Scheme 1, $F_j = 1/n$ (48)], constraints within the oligomer impose a large difference on the dissociation constants of individual sites (i.e., $K_{Pj}/K_{P(j-1)} > 10$); thus, the corresponding value of K_{Pj} exceeds the highest concentration of the radioligand. Since each site functions independently, the affinity of one is unaffected by occupancy of another. Between these extremes are systems in which microscopically dissimilar sites also undergo cooperative transitions. In each case, the possible magnitude of any difference in apparent capacity would depend on the number of sites within the cluster and upon the oligomeric homogeneity of the preparation; that is, there may be a unique oligomeric form (e.g., a tetramer) or a mixture of forms (e.g., dimers and tetramers).

The data in Figure 1A,C can be described in terms of cooperative effects or asymmetry and therefore are mechanistically ambiguous. Cooperativity is favored, however, by the evidence for concomitant binding of two different ligands. The interaction between unlabeled N -methylscopolamine and [^3H]quinuclidinylbenzilate is manifestly inconsistent with Scheme 1 (Table 2), while the agreement with Scheme 2 implies a cooperative effect of one ligand on the binding of the other. If the inhibition of [^3H]quinuclidinylbenzilate by unlabeled N -methylscopolamine is a manifestation of cooperativity between the two ligands, negative cooperativity may determine the level of maximal binding observed at graded concentrations of either radioligand taken alone.

Since N -[^3H]methylscopolamine labeled about 50% of the sites recognized by [^3H]quinuclidinylbenzilate in cholate–NaCl, a divalent receptor is sufficient for cooperativity to account for the data presented in Figure 1A. When the data from Figure 1A are combined with those from Figure 1B, however, an adequate description of both cannot be obtained with only two or three interacting sites (Table 3). The receptor must be at least tetravalent (i.e., Scheme 2) if the agreement is to approach that obtained empirically in terms of Scheme 1 (cf. Figures 1 and 8). A comparable fit requires

six or eight interacting sites (Table 3). It follows that the receptor may exist in clusters comprising as many as eight subunits. Four interacting sites also are required for the pooled data on receptors solubilized in Lubrol-PX (Figure 1C,D) if cooperativity is to yield a sum of squares comparable to that obtained from the empirical analysis in terms of Scheme 1 (Table 3).

Previous reports of cooperative binding to G protein-coupled receptors include the early observation that the dissociation of (–)-[³H]alprenolol from β -adrenergic receptors was faster when initiated by an unlabeled ligand than by dilution (52, 53). In studies conducted at equilibrium, Hill coefficients greater than 1 have raised the possibility of positive cooperativity in the binding of some ligands to cardiac muscarinic and cortical histaminergic receptors (39, 54–56). Also, cooperative interactions have been inferred from the combined effects of two or more ligands on binding to muscarinic receptors from rat adenohypophysis (57) and to histaminergic receptors from rat and guinea pig cortex (58–61); the same data were inconsistent with the notion that the ligands compete for noninteracting sites.

More recent studies have demonstrated that allosteric effects can emerge when pharmacologically distinct receptors are coexpressed, and the heteromeric nature of the putative complex has been confirmed by coimmunoprecipitation. With heterooligomers formed by δ - and κ -opioid receptors, the apparent affinity of the δ -selective agonist [D-Pen²,D-Pen⁵]enkephalin was at least 50-fold higher in the presence of the κ -selective agonist U69593 and vice versa (20). With heterooligomers of the dopamine D₂ and the somatostatin SSTR5 receptors, the affinity of somatostatin-14 was increased 30-fold in the presence of the D₂ agonist quinpirole and decreased 5-fold in the presence of the D₂ antagonist sulpiride (24). Ligands specific for one receptor therefore appear to affect those specific for another in a cooperative manner.

The present results were obtained with a single muscarinic subtype, and similar effects have been reported for the binding of [³H]spiperone and [³H]raclopride to dopamine D₂ receptors expressed in CHO cells (62). In the absence of sodium ions, [³H]raclopride labeled about one-half of the sites recognized by [³H]spiperone; moreover, the binding of [³H]spiperone was inhibited fully by unlabeled raclopride at near-saturating concentrations of the radioligand. The differential capacity and noncompetitive effect were rationalized in terms of negative cooperativity, and it was suggested that a divalent receptor could account for the data.

Evidence for cooperativity also has emerged from studies on cardiac muscarinic receptors that copurify with G proteins. In the presence of GMP-PNP, binding of the antagonist [³H]-AF-DX 384 was found to exhibit a bell-shaped dependence on the concentration of the agonist oxotremorine-M (39). The nucleotide-sensitive effect of agonists on the binding of radiolabeled antagonists to muscarinic receptors generally mirrors the agonist-sensitive effect of GDP on the binding of [³⁵S]GTP γ S to receptor-linked G proteins (34, 46), and the binding profile of GDP also was found to be bell-shaped under some conditions (46). If the system is at equilibrium, such a bell-shaped dependence is indicative of positive cooperativity between the radiolabeled and unlabeled ligands. Cooperative effects imply that multiple states of affinity are intrinsic to the receptor, and heterogeneity has been identified

in the binding of agonists to purified muscarinic receptors from brain (63–65) and heart (33, 39, 66).

The evidence for cooperativity in the binding of agonists and antagonists has implications for the mechanism of signaling in G protein-mediated systems. It suggests that the basic functional unit is a heterooligomeric array comprising two or more equivalents of receptor on one hand and G protein on the other. Within that complex, multiple states of affinity could arise from cooperative interactions between successive equivalents of agonist or antagonist binding to the receptor or between successive equivalents of guanylyl nucleotide binding to the G protein; similarly, the allosteric interactions between agonists and guanylyl nucleotides could arise from effects of one ligand on the degree of cooperativity in the binding of the other (39, 40, 46). Such an arrangement offers an alternative to the view that agonists and guanylyl nucleotides act to shift a ligand-regulated equilibrium between free receptors and G proteins on one hand and a transient RG complex on the other. It has been shown previously that Scheme 2 can describe the nucleotide-sensitive binding of agonists to muscarinic receptors labeled by *N*-[³H]methylscopolamine in ventricular membranes from hamster heart (40). Models with fewer than four interacting sites were inadequate if the radioligand was assumed to label all sites at the apparently saturating concentrations used in the experiments (i.e., $p_j \approx 1$ for all j). The parametric values inferred in terms of Scheme 2 were consistent with the observation that guanylyl nucleotides decrease the apparent capacity for radiolabeled agonists with little or no effect on their affinity (e.g., refs 67–69).

Issues that arise from the suggestion of cooperative effects include the oligomeric stability of the supposed arrays, the number of interacting sites, and the complement of oligomeric forms. It has been assumed, both here and previously (39, 40), that there is only one multivalent form of the receptor in any particular preparation. If the oligomer and its cooperative properties are relevant to signaling, the defined nature of multimeric systems such as hemoglobin, aspartate transcarbamoylase, bacteriorhodopsin, and the nicotinic receptor suggests that the muscarinic receptor exists functionally as a single quaternary species. Other forms may be present, however, and a mixture of different oligomers may behave in a manner that can be described in terms of a tetramer alone.

A mixture of monovalent and tetravalent receptors was required if cooperativity was to account for the binding properties of M₂ muscarinic receptors in membranes from hamster heart (40). The monovalent or noncooperative form represented 5–10% of all sites. A homogeneous population of tetravalent receptors was sufficient to account for the properties of purified M₂ receptors from porcine atria (39), although it seems in retrospect that effects rationalized in terms of cooperativity arose in part from *N*-[³H]methylscopolamine contaminated with scopolamine (48). With the present data from extracts in cholate–NaCl (i.e., Figure 1A,B), the fit of Scheme 2 is only marginally better when a small monovalent population representing 4% of the labeled sites is included in the analysis ($P = 0.01$). The binding properties are therefore consistent with the suggestion that the receptor occurs primarily as an oligomer, at least in myocardial preparations. Studies in mammalian cells have shown that mutant receptors inhibit the surface expression

of the wild-type PAF receptor (28), V2 vasopressin receptor (70), and D₂ dopamine receptor (71). Those observations suggest that oligomerization is a prerequisite for trafficking of the receptor to the cell surface and that any monomers are retained in intracellular compartments.

Studies on *c-myc*- and FLAG-tagged muscarinic receptors expressed in Sf9 cells have confirmed that the M₂ subtype can exist as oligomers (4). The differentially tagged receptors were shown to coimmunoprecipitate when coexpressed and solubilized in digitonin–cholate, Lubrol-PX, or *n*-dodecyl β -D-maltoside. No coimmunoprecipitation occurred with coexpressed receptors solubilized in cholate–NaCl, but the lack of an effect was attributed to the low efficiency of immunoprecipitation observed with the anti-*c-myc* antibody in that detergent. That interpretation has been confirmed in more recent studies, where the two epitopes were coimmunoprecipitated from extracts in cholate–NaCl using antibodies from a different supplier.⁷ The efficiency of immunoprecipitation in digitonin–cholate was high for receptors extracted from coinfecting cells relative to those from cells expressing only the *c-myc*-tagged form, suggesting that the oligomer is trimeric or larger. Also, the failure to effect any change in the level of coimmunoprecipitation indicated that the receptor retained its oligomeric integrity under the conditions of the binding assays, in accord with the assumptions underlying Scheme 2.

The present results indicate that the properties of solubilized M₂ receptors depend in part on the detergent. The overall affinity of the receptor for either *N*-[³H]methylscopolamine or [³H]quinuclidinylbenzilate was similar in digitonin–cholate and cholate–NaCl but much weaker in Lubrol-PX (Table 1). Also, the differential capacity and related noncompetitive effects observed in cholate–NaCl and Lubrol-PX were not found in digitonin–cholate, where the two ligands appear to compete directly for all of the sites. In terms of Scheme 2, receptors in cholate–NaCl or Lubrol-PX on one hand and in digitonin–cholate on the other differ primarily in the values of a_3 and c_j . The supposed oligomer therefore appears to exist in two or more states that differ in their cooperative properties and possibly in the degree of asymmetry among the constituent sites. Since digitonin can recover those sites that are latent upon extraction in cholate–NaCl, the effects of detergents appear to be reversible. It follows that the oligomers can interconvert, at least under some conditions, and that the detergent regulates their distribution among the different states.

The regulatory factors may include the detergent itself, the lipid (or lack thereof) that accompanies the receptor during extraction, or both. In studies on rhodopsin and the 5-HT_{1A} receptor, the quantities of lipid, the ratio of lipid to protein, and the composition of lipids in solubilized extracts all were found to depend on the detergent used to extract the former from photoreceptor disk membranes and the latter from sheep brain gray matter (72, 73). Moreover, the total amount of lipids extracted by digitonin from sheep brain gray matter was found to be much lower than that extracted by sodium cholate or Thesit (73), which is similar in structure to Lubrol-PX.

Detergents are known to affect photocycling in bacteriorhodopsin, which crystallizes as a homotrimer (74). It has

been suggested that cooperativity accounts at least in part for light-dependent effects on the relative amounts of different M intermediates within the photocycle (75). Those effects were eliminated by Triton X-100 at concentrations that did not disrupt the trimeric structure (76), and they were regained upon the addition of specific lipids (77). Also, the photocycle of rhodopsin was arrested at the meta I intermediate in digitonin but continued to the meta II intermediate in *n*-dodecyl β -D-maltoside (78). The meta II state of rhodopsin corresponds to the M form of bacteriorhodopsin (79). Data from FTIR difference spectroscopy suggest that rhodopsin undergoes a change in specific lipid–receptor interactions as a result of conformational changes induced by activation (80). In addition, the downstream interaction between transducin and its effector cGMP phosphodiesterase has been shown to depend on the nature of the lipid environment (81).

In a comparison of muscarinic receptors in cortical and atrial membranes from pig, the antagonist pirenzepine bound 34-fold more tightly to the former than to the latter (82). Such a difference is typical of pirenzepine and generally is attributed to the preponderance of M₂ receptors in the heart on one hand and the comparatively high level of M₁ receptors in the cortex on the other (83). Comparable specificity has been found when each subtype is expressed individually in CHO or Sf9 cells (84–86). The difference in affinity was lost, however, when the cortical and atrial membranes from pig were solubilized and purified in digitonin; moreover, it was recovered when the receptors were reinserted in the original membranes or reconstituted in lipid vesicles (82). A similar reduction in the selectivity of pirenzepine was found with digitonin-solubilized receptors from rat heart (87), where the affinity approximated that measured in membranes or solubilized preparations from cerebral cortex (63).

Recent studies on the IgE receptor have suggested that rafts and raft-like domains play an important role in transmembrane signaling via that system (88). The importance of such microdomains in the mechanism of G protein-mediated signaling is unknown, but M₂ muscarinic receptors, G proteins, and adenylate cyclase all have been shown to be enriched in raft-like domains (89–91). It follows that the lipid composition of microdomains may play a role in signaling through those systems, perhaps by modulating the cooperative properties of the receptor.

ACKNOWLEDGMENT

We are grateful to the managers and staff of Quality Meat Packers Ltd. and the New York Pork and Food Exchange (Toronto) for generous supplies of porcine atria and for their cooperation in allowing immediate access to fresh tissue. We thankfully acknowledge Dr. Tatsuya Haga for helpful discussions and Hui Ha for assistance in the binding assays during the early stages of the investigation.

REFERENCES

1. Hébert, T. E., and Bouvier, M. (1998) *Biochem. Cell Biol.* 76, 1–11.
2. Milligan, G. (2001) *J. Cell Sci.* 114, 1265–1271.
3. Salahpour, A., Angers, S., and Bouvier, M. (2000) *Trends Endocrinol. Metab.* 11, 163–168.
4. Park, P., Sum, C. S., Hampson, D. R., Van Tol, H. H. M., and Wells, J. W. (2001) *Eur. J. Pharmacol.* 421, 11–22.

⁷ Paul S.-H. Park and James W. Wells, unpublished observations.

5. Zeng, F.-Y., and Wess, J. (1999) *J. Biol. Chem.* 274, 19487–19497.
6. Hébert, T. E., Moffett, S., Morello, J.-P., Loisel, T. P., Bichet, D. G., Barret, C., and Bouvier, M. (1996) *J. Biol. Chem.* 271, 16384–16392.
7. Karpa, K. D., Lin, R., Kabbani, N., and Levenson, R. (2000) *Mol. Pharmacol.* 58, 677–683.
8. Cvejic, S., and Devi, L. A. (1997) *J. Biol. Chem.* 272, 26959–26964.
9. Pfeiffer, M., Koch, T., Schröder, H., Klutzny, M., Kirscht, S., Kreienkamp, H.-J., Höllt, V., and Schulz, S. (2001) *J. Biol. Chem.* 276, 14027–14036.
10. Yesilaltay, A., and Jenness, D. D. (2000) *Mol. Biol. Cell* 11, 2873–2884.
11. Rocheville, M., Lange, D. C., Kumar, U., Sasi, R., Patel, R. C., and Patel, Y. C. (2000) *J. Biol. Chem.* 275, 7862–7869.
12. Angers, S., Salahpour, A., Joly, E., Hilairt, S., Chelsky, D., Dennis, M., and Bouvier, M. (2000) *Proc. Natl. Acad. Sci. U.S.A.* 97, 3684–3689.
13. McVey, M., Ramsay, D., Kellett, E., Rees, S., Wilson, S., Pope, A. J., and Milligan, G. (2001) *J. Biol. Chem.* 276, 14092–14099.
14. Overton, M. C., and Blumer, K. J. (2000) *Curr. Biol.* 10, 341–344.
15. Jones, K. A., Borowsky, B., Tamm, J. A., Craig, D. A., Durkin, M. M., Dai, M., Yao, W.-J., Johnson, M., Gunwaldsen, C., Huang, L.-Y., Tang, C., Shen, Q., Salon, J. A., Morse, K., Laz, T., Smith, K. E., Nagarathnam, D., Noble, S. A., Branchek, T. A., and Gerald, C. (1998) *Nature* 396, 674–678.
16. Kaupmann, K., Malitschek, B., Schuler, V., Heid, J., Froestl, W., Beck, P., Mosbacher, J., Bischoff, S., Kulik, A., Shigemoto, R., Karschin, A., and Bettler, B. (1998) *Nature* 396, 683–687.
17. Kuner, R., Köhr, G., Grünewald, S., Eisenhardt, G., Bach, A., and Kornau, H.-C. (1999) *Science* 283, 74–77.
18. Ng, G. Y. K., Clark, J., Coulombe, N., Ethier, N., Hébert, T. E., Sullivan, R., Kargman, S., Chateaufneuf, A., Tsukamoto, N., McDonald, T., Whiting, P., Mezey, E., Johnson, M. P., Liu, Q., Kolakowski, L. F., Evans, J. F., Bonner, T. I., and O'Neill, G. P. (1999) *J. Biol. Chem.* 274, 7607–7610.
19. White, J. H., Wise, A., Main, M. J., Green, A., Fraser, N. J., Disney, G. H., Barnes, A. A., Emson, P., Foord, S. M., and Marshall, F. H. (1998) *Nature* 396, 679–682.
20. Jordan, B. A., and Devi, L. A. (1999) *Nature* 399, 697–700.
21. George, S. R., Fan, T., Xie, Z., Tse, R., Tam, V., Varghese, G., and O'Dowd, B. F. (2000) *J. Biol. Chem.* 275, 26128–26135.
22. AbdAlla, S., Lothar, H., and Quitterer, U. (2000) *Nature* 407, 94–98.
23. Ginés, S., Hillion, J., Torvinen, M., Le Crom, S., Casadó, V., Canela, E. I., Rondin, S., Lew, J. Y., Watson, S., Zoli, M., Agnati, L. F., Vernier, P., Lluís, C., Ferré, S., Fuxe, K., and Franco, R. (2000) *Proc. Natl. Acad. Sci. U.S.A.* 97, 8606–8611.
24. Rocheville, M., Lange, D. C., Kumar, U., Patel, S. C., Patel, R. C., and Patel, Y. C. (2000) *Science* 288, 154–157.
25. Maggio, R., Vogel, Z., and Wess, J. (1993) *Proc. Natl. Acad. Sci. U.S.A.* 90, 3103–3107.
26. Monnot, C., Bihoreau, C., Conchon, S., Curnow, K. M., Corvol, P., and Clauser, E. (1996) *J. Biol. Chem.* 271, 1507–1513.
27. Hébert, T. E., Loisel, T. P., Adam, L., Ethier, N., St. Onge, S., and Bouvier, M. (1998) *Biochem. J.* 330, 287–293.
28. Le Gouill, C., Parent, J.-L., Caron, C.-A., Gaudreau, R., Volkov, L., Rola-Pleszczynski, M., and Staňková, J. (1999) *J. Biol. Chem.* 274, 12548–12554.
29. Birnbaumer, L., Abramowitz, J., and Brown, A. M. (1990) *Biochim. Biophys. Acta* 1031, 163–224.
30. De Lean, A., Stadel, J. M., and Lefkowitz, R. J. (1980) *J. Biol. Chem.* 255, 7108–7117.
31. Gilman, A. G. (1987) *Annu. Rev. Biochem.* 56, 615–649.
32. Samama, P., Cotecchia, S., Costa, T., and Lefkowitz, R. J. (1993) *J. Biol. Chem.* 268, 4625–463624.
33. Ikegaya, T., Nishiyama, T., Haga, K., Haga, T., Ichiyama, A., Kobayashi, A., and Yamazaki, N. (1990) *J. Mol. Cell. Cardiol.* 22, 343–351.
34. Tota, M. R., Kahler, K. R., and Schimerlik, M. I. (1987) *Biochemistry* 26, 8175–8182.
35. Birdsall, N. J. M., Burgen, A. S. V., and Hulme, E. C. (1977) *Adv. Behav. Biol.* 24, 25–33.
36. Ehler, F. J. (1985) *Mol. Pharmacol.* 28, 410–421.
37. Potter, L. T., and Ferrendelli, C. A. (1989) *J. Pharmacol. Exp. Ther.* 248, 974–978.
38. Green, M. A., Chidiac, P., and Wells, J. W. (1997) *Biochemistry* 36, 7380–7394.
39. Wreggett, K. A., and Wells, J. W. (1995) *J. Biol. Chem.* 270, 22488–22499.
40. Chidiac, P., Green, M. A., Pawagi, A. B., and Wells, J. W. (1997) *Biochemistry* 36, 7361–7379.
41. Peterson, G. L., Rosenbaum, L. C., and Schimerlik, M. I. (1988) *Biochem. J.* 255, 553–560.
42. Carson, S. (1982) *Biochem. Pharmacol.* 31, 1806–1809.
43. Wells, J. W. (1992) in *Receptor–Ligand Interactions. A Practical Approach* (Hulme, E. C., Ed.) pp 289–395, Oxford University Press, Oxford.
44. Seeman, P., Ulpian, C., Wreggett, K. A., and Wells, J. W. (1984) *J. Neurochem.* 43, 221–235.
45. Marquardt, D. W. (1963) *J. Soc. Ind. Appl. Math.* 2, 431–441.
46. Chidiac, P., and Wells, J. W. (1992) *Biochemistry* 31, 10908–10921.
47. Waelbroeck, M., Camus, J., Winand, J., and Christophe, J. (1987) *Life Sci.* 41, 2235–2240.
48. Sum, C. S., Pyo, N., and Wells, J. W. (2001) *Biochem. Pharmacol.* 62, 829–851.
49. Hulme, E. C., Birdsall, N. J. M., Burgen, A. S. V., and Mehta, P. (1978) *Mol. Pharmacol.* 14, 737–750.
50. Luetje, C. W., Brunwell, C., Norman, M. G., Peterson, G. L., Schimerlik, M. I., and Nathanson, N. M. (1987) *Biochemistry* 26, 6892–6896.
51. Maeda, A., Kubo, T., Mishina, M., and Numa, S. (1988) *FEBS Lett.* 239, 339–342.
52. Limbird, L. E., De Meyts, P., and Lefkowitz, R. J. (1975) *Biochem. Biophys. Res. Commun.* 64, 1160–1168.
53. Limbird, L. E., and Lefkowitz, R. J. (1976) *J. Biol. Chem.* 251, 5007–5014.
54. Boyer, J. L., Martinez-Carcamo, M., Monroy-Sanchez, J. A., Posadas, C., and Garcia-Sainz, J. A. (1986) *Biochem. Biophys. Res. Commun.* 134, 172–177.
55. Mattera, R., Pitts, B. J. R., Entman, M. L., and Birnbaumer, L. (1985) *J. Biol. Chem.* 260, 7410–7421.
56. Sinkins, W. G., Kandel, M., Kandel, S. I., Schunack, W., and Wells, J. W. (1993) *Mol. Pharmacol.* 43, 569–582.
57. Henis, Y. I., and Sokolovsky, M. (1983) *Mol. Pharmacol.* 24, 357–365.
58. Steinberg, G. H., Eppel, J. G., Kandel, M., Kandel, S. I., and Wells, J. W. (1985) *Biochemistry* 24, 6095–6107.
59. Steinberg, G. H., Kandel, M., Kandel, S. I., and Wells, J. W. (1985) *Biochemistry* 24, 6107–6115.
60. Steinberg, G. H., Kandel, M., Kandel, S. I., and Wells, J. W. (1985) *Biochemistry* 24, 6115–6125.
61. Sinkins, W. G., and Wells, J. W. (1993) *Mol. Pharmacol.* 43, 583–594.
62. Armstrong, D., and Strange, P. G. (2001) *J. Biol. Chem.* 276, 22621–22629.
63. Berrie, C. P., Birdsall, N. J. M., Dadi, H. K., Hulme, E. C., Morris, R. J., Stockton, J. M., and Wheatley, M. (1985) *Trans. Biochem. Soc.* 13, 1101–1103.
64. Bernstein, G., Haga, K., Haga, T., and Ichiyama, A. (1988) *J. Neurochem.* 50, 1687–1694.
65. Haga, K., Haga, T., and Ichiyama, A. (1986) *J. Biol. Chem.* 261, 10133–10140.
66. Peterson, G. L., Herron, G. S., Yamaki, M., Fullerton, D. S., and Schimerlik, M. I. (1984) *Proc. Natl. Acad. Sci. U.S.A.* 81, 4993–4997.
67. Galper, J. B., Haigh, L. S., Hart, A. C., O'Hara, D. S., and Livingston, D. J. (1987) *Mol. Pharmacol.* 32, 230–240.

68. Gurwitz, D., Kloog, Y., and Sokolovsky, M. (1985) *Mol. Pharmacol.* 28, 297–305.
69. Harden, T. K., Meeker, R. B., and Martin, M. W. (1983) *J. Pharmacol. Exp. Ther.* 227, 570–577.
70. Zhu, X., and Wess, J. (1998) *Biochemistry* 37, 15773–15784.
71. Lee, S. P., O'Dowd, B. F., Ng, G. Y. K., Varghese, G., Akil, H., Mansour, A., Nguyen, T., and George, S. R. (2000) *Mol. Pharmacol.* 58, 120–128.
72. Aveldano, M. I. (1995) *Arch. Biochem. Biophys.* 324, 331–343.
73. Banerjee, P., Joo, J. B., Buse, J. T., and Dawson, G. (1995) *Chem. Phys. Lipids* 77, 65–78.
74. Pebay-Peyroula, E., Rummel, G., Rosenbusch, J. P., and Landau, E. M. (1997) *Science* 277, 1676–1681.
75. Schragar, R. I., Hendler, R. W., and Bose, S. (1995) *Eur. J. Biochem.* 229, 589–595.
76. Mukhopadhyay, A. K., Dracheva, S., Bose, S., and Hendler, R. W. (1996) *Biochemistry* 35, 9245–9252.
77. Joshi, M. K., Dracheva, S., Mukhopadhyay, A. K., Bose, S., and Hendler, R. W. (1998) *Biochemistry* 37, 14463–14470.
78. Resek, J. F., Farahbakhsh, Z. T., Hubbell, W. L., and Khorana, H. G. (1993) *Biochemistry* 32, 12025–12032.
79. Behrens, W., Alexiev, U., Mollaaghababa, R., Khorana, H. G., and Heyn, M. P. (1998) *Biochemistry* 37, 10411–10419.
80. Isele, J., Sakmar, T. P., and Siebert, F. (2000) *Biophys. J.* 79, 3063–3071.
81. Melia, T. J., Malinski, J. A., He, F., and Wensel, T. G. (2000) *J. Biol. Chem.* 275, 3535–3542.
82. Berstein, G., Haga, T., and Ichiyama, A. (1989) *Mol. Pharmacol.* 36, 601–607.
83. Hammer, R. (1989) *Prog. Pharmacol. Clin. Pharmacol.* 7/1, 1–11.
84. Buckley, N. J., Bonner, T. I., Buckley, C. M., and Brann, M. R. (1989) *Mol. Pharmacol.* 35, 469–476.
85. Dong, G. Z., Kameyama, K., Rinken, A. and Haga, T. (1995) *J. Pharmacol. Exp. Ther.* 274, 378–384.
86. Dörje, F., Wess, J., Lambrecht, G., Tacke, R., Mutschler, E., and Brann, M. R. (1991) *Mol. Pharmacol.* 256, 727–733.
87. Birdsall, N. J. M., Hulme, E. C., and Keen, M. (1986) *Br. J. Pharmacol.* 87, 307–316.
88. Brown, D. A., and London, E. (1998) *Annu. Rev. Cell Dev. Biol.* 14, 111–136.
89. Feron, O., Smith, T. W., Michel, T., and Kelly, R. A. (1997) *J. Biol. Chem.* 272, 17744–17748.
90. Huang, C., Hepler, J. R., Chen, L. T., Gilman, A. G., Anderson, R. G. W., and Mumby, S. M. (1997) *Mol. Biol. Cell* 8, 2365–2378.
91. Wu, C., Butz, S., Ying, Y., and Anderson, R. G. W. (1997) *J. Biol. Chem.* 272, 3554–3559.

BI011746S